

# **SWIPT Enabled Full-Duplex Overlay Cognitive NOMA With Hardware Impairments**

**M.Tech. Thesis**

By  
**ANUBHI SINGH**



**DEPARTMENT OF ELECTRICAL ENGINEERING  
INDIAN INSTITUTE OF TECHNOLOGY INDORE  
NOVEMBER 2023**

# **SWIPT Enabled Full-Duplex Overlay Cognitive NOMA With Hardware Impairments**

**A THESIS**

*Submitted in partial fulfillment of the  
requirements for the award of the degree  
of*  
**Master of Technology**

*by*  
**ANUBHI SINGH**



**DEPARTMENT OF ELECTRICAL ENGINEERING  
INDIAN INSTITUTE OF TECHNOLOGY INDORE  
NOVEMBER 2023**



# INDIAN INSTITUTE OF TECHNOLOGY INDORE

## CANDIDATE'S DECLARATION

I hereby certify that the work which is being presented in the thesis entitled **SWIPT Enabled Full-Duplex Overlay Cognitive NOMA With Hardware Impairments** in the partial fulfillment of the requirements for the award of the degree of **MASTER OF TECHNOLOGY** and submitted in the **DISCIPLINE OF ELECTRICAL ENGINEERING, Indian Institute of Technology Indore**, is an authentic record of my own work carried out during the time period from August 2021 to November 2023 under the supervision of Prof. Prabhat Kumar Upadhyay.

The matter presented in this thesis has not been submitted by me for the award of any other degree of this or any other institute.

Anubhi  
20/11/23

Signature of the student with date  
(ANUBHI SINGH)

-----  
This is to certify that the above statement made by the candidate is correct to the best of my/our knowledge.

24-11-2023

Signature of the Supervisor of  
M.Tech.thesis (with date)  
(Prof. Prabhat Kumar Upadhyay)

-----  
ANUBHI SINGH has successfully given his/her M.Tech. Oral Examination held on **NOVEMBER 15<sup>th</sup> 2023**.

Signature(s) of Supervisor(s) of M.Tech. thesis  
Date: 24-11-2023

Convener, DPGC  
Date: 26/11/2023

Bodhisatwa Mazumdar

Signature of PSPC Member #1  
Date: 26-11-2023

Signature of PSPC Member #2  
Date: 26/11/2023

## ACKNOWLEDGEMENTS

I would like to express my sincere gratitude to all those who have supported and contributed to the completion of this Master's thesis. Without their assistance, guidance, and encouragement, this research would not have been possible. First and foremost, I am deeply grateful to almighty GOD and to my supervisor, **Prof. Prabhat K. Upadhyay**, for his continuous support throughout the entire research process. I am indebted to **Dr. Chandan Kumar Singh**, for being an instrumental for my work. I appreciate them for their invaluable and thorough guidance during the course of my thesis. The unwavering commitment to excellence, patience, and insightful feedback played a significant role in shaping this thesis. I would also like to extend my appreciation to the faculty members and academic staff at **Indian Institute of Technology, Indore**, particularly the **Department of Electrical Engineering**, for offering valuable resources that enhanced the quality of my study. Their dedication to fostering an atmosphere of academic rigor and intellectual growth has been instrumental in my personal and professional development. Furthermore, I am grateful to my lab mates, friends and colleagues who have provided support and encouragement throughout this demanding academic journey. Their unwavering belief in my abilities and their willingness to lend an ear or provide advice have been a constant source of inspiration. Lastly, I would like to express my deepest appreciation to my family. Their unconditional love, understanding, and encouragement have been my pillars of strength throughout my academic pursuits. Their sacrifices and belief in my potential have been the driving force behind my achievements.

In conclusion, I am humbled and honored to have received support from all these individuals and institutions. Their contributions have been invaluable, and I am truly grateful and indebted for their involvement in this research endeavor.

## Abstract

Wireless system energy and spectrum efficiency can be increased by combining energy harvesting using cognitive radio with Non-orthogonal Multiple Access (NOMA) approaches. In this thesis, we analyze the performance of an overlay cognitive multiuser NOMA (OCNOMA) system in the presence of Hardware Impairments (HIs) on its transceiver nodes. The major transmitter's radio frequency signal is harvested by an energy-constrained full duplex secondary transmitter node, which then uses that energy to send its own unique communication signal using the NOMA technique in addition to relaying the primary information signal. We use the Spectrum Sharing Cooperation-Decode and Forward (SSC-DF) protocol for this purpose. Crucially, we take into account the effects of noisy signal processing caused by HIs and inadequate sequential interference cancellation in NOMA, both of them are inevitable in systems found in the real world. Additionally, we address the DPT (Direct Primary Transmission) scheme as a benchmark for evaluating the effectiveness of the full-duplex (FD) based cooperative spectrum sharing transmission (CSST) scheme. We uncover some relevant ceiling effects in the system by obtaining the mathematical equations of outage probability of the primary and secondary networks. In addition, we assess the energy efficiency and system throughput of the OCNOMA system under consideration. Our findings show off the advantages of the recommended SWIPT enabled FD CSST technique over the standard orthogonal multiple access and its half-duplex (HD) counterparts.

# TABLE OF CONTENTS

<b>Chapter 1</b> .....	1
INTRODUCTION.....	1
1.1 Problem Statement.....	2
1.2 Thesis Outline.....	3
<b>Chapter 2</b> .....	4
REVIEW OF PAST WORK AND PROBLEM FORMULATION .....	4
2.1 Literature Survey.....	4
2.2 Problem Formulation.....	6
<b>Chapter 3</b> .....	8
BACKGROUND .....	8
3.1 Cognitive Radio .....	8
3.2 Non Orthogonal Multiple Access.....	10
3.3 Energy Harvesting (EH).....	11
3.3.1 System Imperfections .....	11
3.3.2 SWIPT.....	12
<b>Chapter 4</b> .....	14
HALF DUPLEX OVERLAY COGNITIVE NOMA SYSTEMS .....	14
4.1 System Description.....	15
4.1.1 System and Channel Models.....	15
4.1.2 EH Phase .....	16
4.1.3 IP Phase.....	16
4.1.4 DF Relaying Strategy.....	17

4.2	Performance Analysis of Primary Network.....	19
4.2.1	DPT Scheme .....	19
4.2.2	SSC Scheme.....	20
4.2.3	Ceiling Effect.....	20
4.3.	Performance Analysis of Secondary Network.....	21
4.3.1	SSC- DF Scheme .....	21
4.3.2	Ceiling Effect .....	22
4.4	Overall OCNOMA System Performance .....	22
4.4.1	System Throughput .....	22
4.4.2	Energy Efficiency.....	22
<b>Chapter 5</b> .....		<b>24</b>
FULL DUPLEX OVERLAY COGNITIVE SYSTEMS.....		24
5.1	Description of Signal and System Models.....	24
5.2	Description of CSST Scheme .....	27
5.3	Performance Analysis of Primary Network.....	30
5.4	Performance Analysis of Secondary Network .....	32
5.5	Overall FD OCNOMA System Performance.....	33
<b>Chapter 6</b> .....		<b>35</b>
RESULTS AND DISCUSSIONS.....		35
<b>Chapter 7</b> .....		<b>41</b>
CONCLUSIONS AND FUTURE WORKS.....		41
REFERENCES.....		42

## LIST OF FIGURES

Sr. No.	Title	Pg. No.
1)	Technology Evolution from 1G to 6G	8
2)	Cognitive Radio Types	9
3)	Basic Diagram of NOMA	10
4)	SWIPT via Static and Mobile Base Stations	13
5)	SWIPT Transmission Technique in Different Domains	13
6)	OCNOMA system model.	14
7)	Block Structure of EH-based OCNOMA System for Transmission	14
8)	System Model for FD OCNOMA	24
9)	Transmission block using TS-based EH protocol for the FD OCNOMA system	26
10)	Transmission block with PS-based EH protocol for the FD OCNOMA system	28
11)	OP vs SNR for under TS protocol for primary network	36
12)	OP vs SNR for under PS protocol for primary network	36
13)	OP vs SNR of secondary network for the two-users	37
14)	OP vs SNR under TS protocol secondary user ( $U_1$ )	38
15)	OP vs SNR under TS protocol secondary user ( $U_2$ )	38
16)	Plots of throughput vs SNR for the FD OCNOMA system	39
17)	Plots of Energy efficiency vs SNR for FD OCNOMA system	40

# Abbreviations

<b>1G</b>	<b>First-Generation</b>
<b>5G</b>	<b>Fifth-Generation</b>
<b>AWGN</b>	<b>Additive White Gaussian Noise</b>
<b>CDF</b>	<b>Cumulative Distribution Function</b>
<b>C-NOMA</b>	<b>Cooperative NOMA</b>
<b>CR</b>	<b>Cognitive Radio</b>
<b>CR-NOMA</b>	<b>Cognitive NOMA</b>
<b>EH</b>	<b>Energy Harvesting</b>
<b>EVM</b>	<b>Error Vector Magnitude</b>
<b>FD</b>	<b>Full-Duplex</b>
<b>FR</b>	<b>Fixed Relaying</b>
<b>HD</b>	<b>Half-Duplex</b>
<b>HIs</b>	<b>Hardware Impairments</b>
<b>IoT</b>	<b>Internet of Things</b>
<b>IP</b>	<b>Information Processing</b>
<b>I-SIC</b>	<b>Imperfect SIC</b>
<b>LoS</b>	<b>Line-of-Sight</b>
<b>ML</b>	<b>Machine Learning</b>
<b>MRC</b>	<b>Maximal Ratio Combining</b>
<b>NOMA</b>	<b>Non-Orthogonal Multiple Access</b>
<b>OCNOMA</b>	<b>Overlay CR-NOMA</b>
<b>OMA</b>	<b>Orthogonal Multiple Access</b>
<b>OP</b>	<b>Outage Probability</b>
<b>PDF</b>	<b>Probability Density Function</b>
<b>DPT</b>	<b>Direct Primary Transmission</b>
<b>PR</b>	<b>Primary Receiver</b>
<b>P-SIC</b>	<b>Perfect SIC</b>
<b>PS</b>	<b>Power-Splitting</b>
<b>PT</b>	<b>Primary Transmitter</b>
<b>PU</b>	<b>Primary User</b>
<b>QoS</b>	<b>Quality-of-Service</b>
<b>RF</b>	<b>Radio-Frequency</b>

<b>RIS</b>	<b>Reconfigurable Intelligent Surface</b>
<b>SE</b>	<b>Spectral-Efficiency</b>
<b>SIC</b>	<b>Successive Interference Cancellation</b>
<b>SINR</b>	<b>Signal-to-Interference-Plus-Noise Ratio</b>
<b>SNDR</b>	<b>Signal-to-Noise-and-Distortion Ratio</b>
<b>SNR</b>	<b>Signal-to-Noise Ratio</b>
<b>SR</b>	<b>Secondary Receiver</b>
<b>SSC</b>	<b>Spectrum Sharing Cooperation</b>
<b>ST</b>	<b>Secondary Transmitter</b>
<b>SU</b>	<b>Secondary User</b>
<b>SWIPT</b>	<b>Simultaneous Wireless Information Power Transfer</b>
<b>TS</b>	<b>Time-Switching</b>

# Chapter 1

## INTRODUCTION

The increase in mobile data traffic contributes to the analysis of energy as well as spectrum-efficient communication techniques in fifth-generation and subsequent-generation wireless networks [1]. As there is not much spectrum available, it must be used effectively and efficiently in order to meet customer expectations [2]. In today's scenario spectrum efficient communication techniques has given top priority because of the need for high data transmission rates, improved service quality, connected communication equipment, etc.

In addition to spectrum efficiency, energy efficiency has grown in importance as wireless networks develop in the near future [3]. Concerns about energy consumption increase when a gadget is located far away and lacks a consistent power source. These problems can be successfully handled by the technology known as simultaneous wireless information and power transfer, or SWIPT, which allows wireless devices to process information (IP) and harvest energy from radio-frequency (RF) signals at the same time [4]. Two schemes are used to realize SWIPT: time switching (TS) and power splitting (PS) [5]. Some of the received power is used for energy harvesting and the rest is used for information processing in PS-based SWIPT, whereas in TS-based SWIPT, the time is alternated between the energy harvesting and information processing phases [6]. In this thesis we have used TS based SWIPT.

One method for controlling expanding mobile apps over constrained spectrum resources is cognitive radio (CR) [7]. Under the three spectrum access paradigms of interweave, underlay, and overlay, it increases the overall spectrum efficacy of wireless networks [8]. Although primary users (PU) and secondary users (SU) can transmit synchronous data over the same frequency band using both the overlay and underlay models, the interweave model requires spectrum monitoring and spectrum access [9]. With the overlay technique, SU works as relay on priority basis to help the PU communicate, and in return, SU receives access to the PU's spectrum, whereas in the underlay approach, SU delivers data towards its destination [10]. In this project we have used overlay cognitive radio approach.

The technology known as NOMA [13] enables the effective use of available spectrum resources in 5G and future generations. Thanks to NOMA, multiple users can share the same time or frequency band while be multiplexed in the power domain. It utilizes SIC (successive

interference cancellation) on the receiver side and superposition coding on transmitter side to demultiplex the superimposed signals [14]. The combination of NOMA with CR, known as cognitive NOMA, has provided the best way to increase wireless network spectrum efficiency [15].

In this thesis, we will use all these above discussed techniques. Firstly, we will understand the HD overlay cognitive NOMA with single primary and secondary user. Afterwards we will analyse the full duplex overlay cognitive NOMA system with multiple secondary nodes in presence of imperfect SIC and HIs. Here we have used SSC DF relaying strategy. Then we address the PDT scheme as a benchmark for evaluating the effectiveness of the FD based cooperative spectrum sharing transmission (CSST) scheme. We also compare FD -CSST scheme with Direct Transmission link and its HD counterparts by plotting several graphs which are present in Chapter 6.

## **1.1 Problem Statement**

The significant increase in data traffic resulting from the use of mobile applications and how many facets of daily life they touch demands the implementation of contemporary wireless networks. When implementing next-generation communication networks, the most important factors to consider are wide coverage, low signal latency, high-speed internet access, huge capacity, and prolonged battery life.

Regarding this, cognitive radio and non-orthogonal multiple access (NOMA) have emerged as feasible approaches to provide future wireless networks with high throughput and wide coverage. As transceiver nodes have imperfect successive interference cancellation and HIs, in their presence this thesis evaluates the functioning of an overlay cognitive non-orthogonal multiple access (OCNOMA) system using SWIPT technology. It uses spectrum sharing cooperation decode and forward relaying (SSC-DF) method.

Here, using SWIPT technique, a secondary transmitter (ST) node having limited energy utilizes energy from the primary transmitter's (PT) radio-frequency (RF) signal and then use this energy to convey both the primary information signal and its own information signal. ST works as relay and use OCONOMA to transmit its own signal as well as signal of PT. Primary transmitter harness the benefit of diversity here. We have considered two cases. In the first case

ST is half duplex and we have single SU whereas in the second case SU is FD with multiple secondary nodes. For both cases, we have used the SSC-DF scheme.

We also analyse the energy efficiency and system throughput of the OCNOMA system under consideration. Our findings suggest the advantages of the FD-CSST technique over direct transmission link and its half-duplex counterpart.

## **1.2 Thesis Outline**

**Chapter 1** has given a basic introduction to the need for energy-efficient communication techniques, and the objective of the work in brief.

The remaining contents are as follows:

**Chapter 2:** This chapter contains a review of past work done in the domain of efficient communication technics using NOMA and CR and it widely describes the problem statement.

**Chapter 3:** This chapter provides background and details about the fundamentals of basics of SWIPT, NOMA, CR, etc.

**Chapter 4:** This chapter provides background and details about the fundamentals of Half Duplex necessary to understand and proper working of the system models.

**Chapter 5:** This chapter provides details of FD system, various schemes, and mathematical analysis necessary for the results.

**Chapter 6:** This chapter covers experimental results and discussions of the proposed thesis work.

**Chapter 7:** In this chapter, conclusions are made, and a discussion on the possibility of future work is presented.

## Chapter 2

### REVIEW OF PAST WORK AND PROBLEM FORMULATION

#### 2.1 Literature Survey

The rapid expansion of mobile data traffic motivates research on spectral- and energy efficient communication strategies for fifth-generation (5G) and beyond fifth generation (B5G) wireless networks. Various researches had been performed by researchers in past which are presented in this segment.

In 2017, Zhong Xiang Wei and other researchers given a thorough analysis of FD relay systems with the assistance of wireless power transfer (WPT), highlighting two difficulties with implementation: excessive power consumption and FD realization [16].

In 2016, Xun Guan and other scientists suggested that NOMA clearly offers a good compromise between fairness and throughput for visible light-based communication (VLC). This work provides a phase pre-distortion approach to improve the symbol error rate efficiency of NOMA uplink system with successive interference cancellation (SIC) [17].

In 2020 Azar Hakimi et al. examined the performance of NOMA cognitive relay system: A multi-antenna full-duplex cognitive transmitter interacts with a cognitive receiver while simultaneously addressing the NOMA idea in order to facilitate the transmission of a wirelessly powered main transmitter to its matching receiver. He investigates a realistic non-linear energy harvesting (EH) model. Within the restriction that the primary network's rate remains above a specific threshold, they suggest the best possible beamforming architecture for the cognitive transmitter with the objective to optimize the cognitive network's rate. The suggested optimization can significantly expand the rate region towards primary and secondary networks, according to results. Additionally, for the purpose to figure out the network delay-constrained throughput, outage probability formulas for primary and secondary networks that take into account a sub-optimal zero-forcing based beamforming method are generated. Their findings indicate that traditional linear EH model may result in performance issues because the collected power saturates at high transmitted power levels and the harvesting operation requires the least amount of power possible. This mismatches for realistic non-linear EH circuits in the domains of both high and low transmit power [18].

Research communities have paid close attention to SWIPT and NOMA schemes incorporated with CR communication in IoT networks. In order to facilitate D2D (device-to-device) communications with twin batteries in heterogeneous wireless networks for the Internet of Things, researchers in [19] examined an overlay green relay. In order to serve Internet of Things applications, a mm Wave-NOMA dependent relaying method with SWIPT was presented in [20]. The topic of energy-efficient allocation of resources for a cellular network with machine-to-machine (M2M) capabilities is covered by the authors in [21]. As a result, it is stressed that for IoT to work, D2D technology or M2M communications with cellular systems must be anticipated. Using the TS protocol to harvest energy, authors in [22] investigated an overlay spectrum sharing method for SWIPT assisted cognitive IoT networks. To increase average throughput and outage performance, a retransmission technique for SWIPT-based overlay cognitive relay systems has been presented in [23]. The cooperative spectrum sharing techniques known as SWIPT were examined in [24]. By serving as relays for orthogonal frequency division multiplexing and utilizing the energy from the received radio frequency signal, the SUs are able to access the primary spectrum in this manner.

SWIPT has been integrated into the cognitive NOMA systems in several other works. In particular, an interwoven CR-NOMA system with an EH enabled transmit node was explored in [25], where wireless power transfer was accomplished using the out-of-band transmission mode. In [26], the safe energy efficiency optimization problem for a secondary network was addressed and an underlay cognitive NOMA system was investigated.

In [27] the authors studied an overlay CR system in which a main transmitter's (PT) radio frequency signal is used to harvest energy by STs. The ST acts as the main system's DF relaying provider and broadcasts its own data via downlink NOMA. The outage performance of an underlay cooperative NOMA network with SWIPT, in which the fixed power allocation scheme is utilized for the NOMA protocol and the cognitive relay uses the PS scheme to harvest transmission power from the ST, has been studied by authors in [28]. In [29], TS protocol-based power beacon-assisted NOMA was examined by allowing cellular networks and Internet of Things connections to coexist.

Work in recent time [30] has examined FD communications utilizing SWIPT and NOMA schemes in IoT networks, despite the majority of earlier efforts using HD communications. The authors in [31] looked at the beam forming and resource allocation problems for multi-user FD

wireless powered communications. With the assistance of an SU, a PU communicates with the BS in an FD supportive NOMA method that uses spectrum sensing that was reviewed in [32] in order to utilize both unused and insufficiently utilized spectrum resources. A cooperative overlay spectrum sharing network supported by NOMA has been examined in, where SUs can harvest energy and investigate a spectrum access opportunity in exchange for the PT's information being relayed by an FD relaying based ST. It examined the SWIPT protocol based on PS without a primary communication that is direct. The open technical literature has not thoroughly examined the SWIPT-enabled FD NOMA scheme for an overlay cognitive IoT network.

## **2.2 Problem Formulation**

Future wireless networks, including 5G and B5G, will need to take into account important design goals like wide coverage, smooth data transfer, and spectral efficiency (SE). Increased SE can be achieved by applying the promising CR technology to solve the problem of spectrum underutilization. Therefore, CR technique integration into NOMA can greatly improve the operational efficiency of next-generation wireless networks. Cognitive radio NOMA (CR-NOMA) is the process of incorporating NOMA with CR. It has been shown as an effective strategy for improving SE reliability and performance. Thus far, several research works have examined CR-NOMA systems using the underlay and overlay models. Unlike the underlay CR-NOMA model, the overlay CR-NOMA (OCNOMA) model communicates with an SU using the NOMA by using a secondary transmitter (ST) as a PU relay. Spectrum efficiency is sacrificed in the previously mentioned work to achieve the improved OP performance because an HD relay cooperation mode requires more time resources. While C-NOMA can benefit remote users in terms of performance, it also raises system bandwidth expenses. FD relay mechanism is a promising workable way to deal with such problems [12]. Their ability to concurrently receive and broadcast data in the same frequency range, FD relays seeks a good amount of attention from researchers looking to design more SE systems. In this thesis we assessed FD cooperative relaying in conjunction with an energy harvesting (EH) and evaluated the throughput and OP of the NOMA system with multiple user nodes. Greater energy efficiency can be achieved in HD/FD OCNOMA relaying transmission networks by using SWIPT technology. Moreover, while residual loop self-interference (LI) decreases the overall signal-to-interference plus noise ratio (SINR), FD relaying can increase the SE of an OCNOMA system; hence, a trade-off must be made between the system's increasing SE and

deteriorating performance. In addition, the primary causes of HIs in RF transceivers are phase noises, imbalances in the I/Q ratio, and amplifier non-linearities.

In this thesis, we investigate the SWIPT enabled FD OCNOMA system based on CSST scheme with multiple user nodes in the presence of Ip SIC and HIs in order to achieve the objective of designing of future wireless networks.

## Chapter 3

### BACKGROUND

Installing modern wireless networks is necessary to manage the exponentially growing data traffic brought on by the widespread usage of smartphone and tablet applications and their incorporation into many aspects of daily life. First-generation (1G) wireless communication technology has already given way to fifth-generation (5G) technology. When building next-generation communication networks, the most important factors to consider are wide coverage, low signal latency, high-speed internet access, huge capacity, and prolonged battery life.

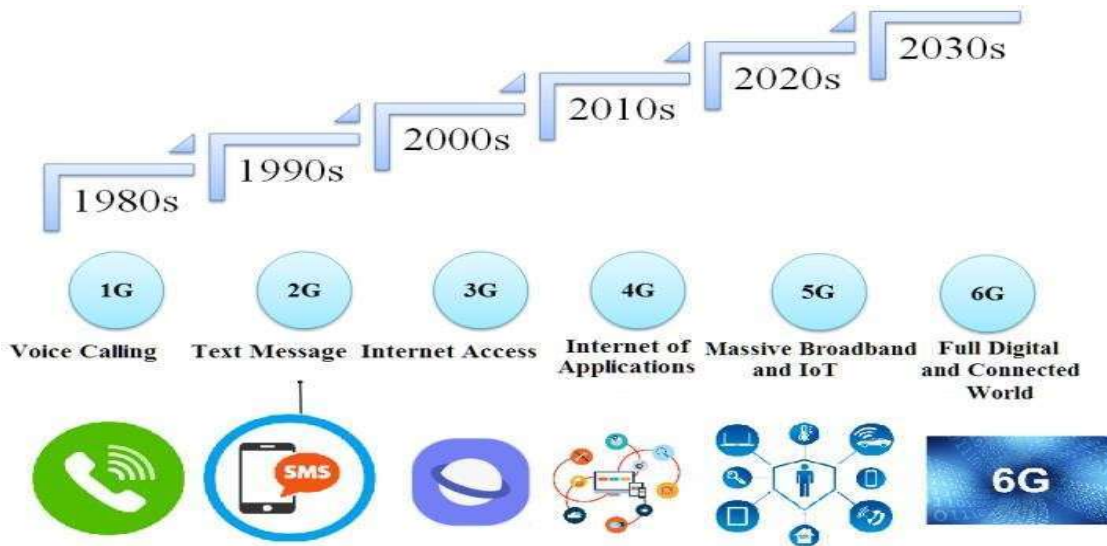


Figure 1: Technology Evolution from 1G to 6G

### 3.1 Cognitive Radio

Wireless communication networks have used cognitive radio (CR) technology to solve spectrum scarcity issues. Sharing spectrum with licensed primary users (PUs) is advantageous for unlicensed secondary users (SUs) in CR networks, provided that doing so does not degrade the primary network's quality-of-service (QoS). The three fundamental forms of spectrum sharing are underlay, overlay, and interweave paradigms.

**Interweave Approach:** By using the interweave technique, the SU can use the PUs' white spaces, or vacant spectrum, opportunistically without disturbing with their transmission. The main drawback of this strategy is that because the SUs must detect the spectrum hole before transmission, they are extremely susceptible to errors in spectrum sensing and principal traffic behavior. Due to a paucity of available spectrum holes, this strategy might not be appropriate for dense networks.

**Underlay Approach:** If SUs meet the interference power criterion (also referred to as the interference temperature limit) toward PUs, they are permitted to share their available spectrum with PUs in underlay method. SUs can directly occupy licensed spectrum using the underlay approach, which has an advantage over the interweave model in that it does not consider the traffic patterns of PUs. Nevertheless, the SUs need to gather the channel status information (CSI) of the pertinent links to the PUs in order to modify their transmission power. In this paradigm, improving SU performance is critical and challenging due to the limiting power at SUs.

**Overlay Approach:** In this strategy, SUs may be given permission to use the PUs' spectrum in exchange for helping the PUs deliver their messages on a priority basis. Because of this, unlike the underlay method, the overlay approach does not impose strict transmit Power constraints on SUs.

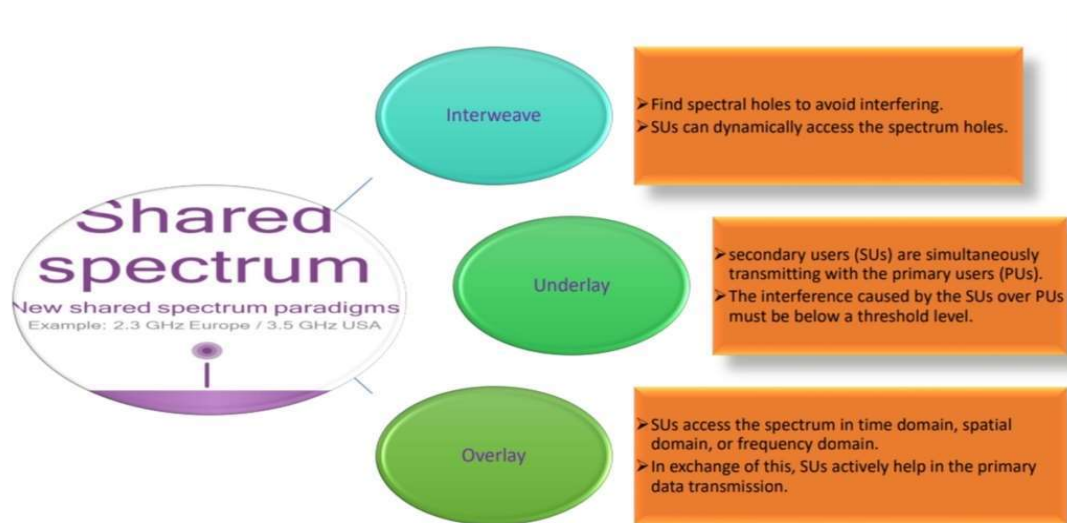


**Figure 2: Cognitive Radio Types**

### 3.2 Non-Orthogonal Multiple Access

Huge connectivity and superior SE are requirements that future wireless communication systems must successfully meet. In this regard, the non-orthogonal multiple access (NOMA) system is among the most promising technologies for future-oriented wireless networks. The basic principle of NOMA is to accommodate multiple users at the transmitter side simultaneously by superimposing and allocating varying degrees of power for every user within the identical time/frequency resources. The desired signals are then decoded on the receiver side using the successive interference cancellation (SIC) process. While waiting for a better connection, the cooperative relaying approach is added to the original NOMA technique to give a spatial diversity gain for the distant NOMA user. Cooperative NOMA (C-NOMA) is the name given to this technique. Here, information from a distant NOMA user can be recognized by a nearby NOMA user with a better link quality, and the nearby user can then serve as a relay to transmit the information during the cooperative phase. This way, the desired signals are received by the far user in duplicate—one from the nearby user's signal and the other from the base station (BS). Combining both of these versions can improve the distant NOMA user's reliability by reaping the rewards from gains in spatial diversity.

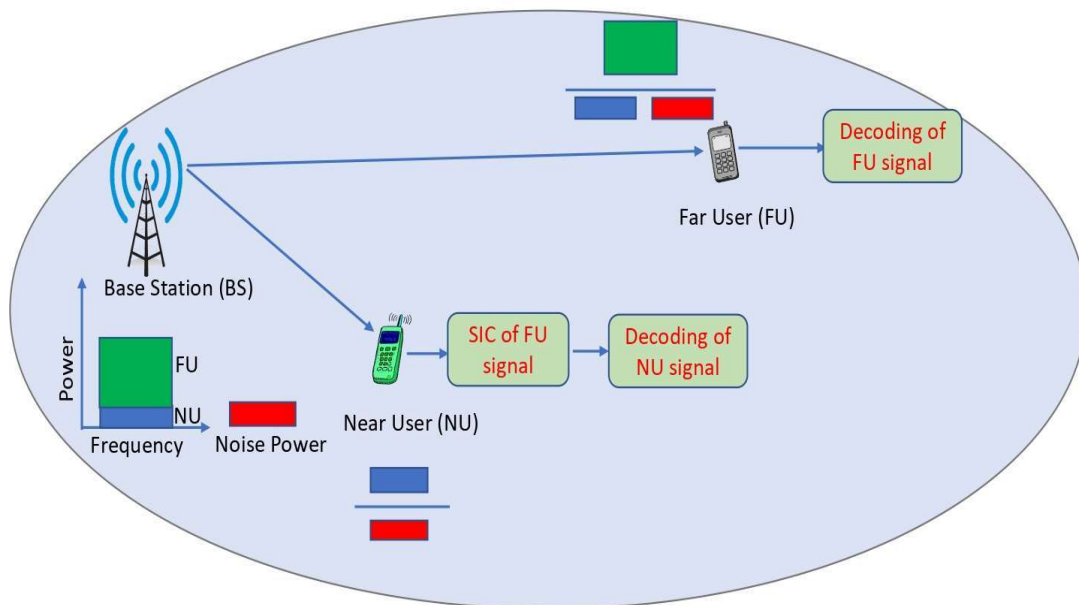


Figure 3: Basic Diagram of NOMA

### 3.3 RF Energy Harvesting (EH)

It is a technique used to capture and convert ambient RF signals, such as Wi-Fi, Bluetooth, and cellular signals, into usable electrical power. Low-power wireless devices, including wearables, sensors, and Internet of Things devices, can be powered by the harvested energy, which operate in remote or inaccessible locations. RF energy harvesting has become an increasingly popular technique in wireless communication due to the abundance of ambient RF signals in the environment and the growing demand for low-power wireless devices. The RF energy harvesting process involves three main components: an antenna, a rectifier, and a storage element. The antenna captures the RF signals from the environment and converts them into electrical signals. The rectifier then converts the AC signals into DC signals, which are more suitable for charging the storage element, such as a battery or a capacitor. The storage element stores the harvested energy for later use by the wireless device. The efficiency of RF energy harvesting depends on several factors, such as the frequency and power level of the ambient RF signals, the size and quality of the antenna, and the efficiency of the rectifier and storage element. The efficiency can range from a few percent to tens of percent, depending on the application requirements and the present energy in that particular environment. There are several challenges associated with RF energy harvesting, such as the variability of the ambient RF signals, the interference from other RF devices, and the distance between the wireless device and the energy source. To overcome these challenges, researchers are developing new techniques and technologies, such as multiband antennas, adaptive rectifiers, and power management circuits, to improve the efficiency and reliability of RF energy harvesting.

### 3.4 System Imperfections

System imperfections refer to the limitations or constraints that affect the performance of a communication system. Imperfections can arise due to various factors such as hardware limitations, environmental factors, or design choices. Three broad categories can be used to classify imperfections in general. They are channel imperfections, hardware imperfections, and algorithmic imperfections.

**1. Channel Imperfections:** The channel is the means for exchange between the sender and the person who receives that information. However, due to environmental factors and other limitations, the channel is never perfect, and its imperfections can affect system performance. Some common types of channel imperfections include fading, interference, noise.

**2. Hardware Imperfections:** Hardware imperfections refer to the limitations of the physical components used in the communication system. Hardware imperfections can be due to several factors such as limitations of the electronic components, power amplifiers, filters, and antennas. Some common types of hardware imperfections include nonlinear distortion, frequency offset, phase noise.

**3. Algorithmic Imperfections:** Algorithmic imperfections refer to the limitations of the signal processing algorithms used in the communication system. Algorithmic imperfections can be due to various factors such as suboptimal algorithms, poor parameter estimation, or design choices. Some common types of algorithmic imperfections include channel estimation errors, timing errors, power allocation errors.

In conclusion, system imperfections can arise due to various factors, and their impact on the system performance can be significant. Understanding and mitigating these imperfections is critical to achieving optimal performance in communication systems.

### **3.5 Simultaneous Wireless Information and Power Transfer (SWIPT)**

An encouraging technique that makes use of radio frequency energy is SWIPT, which combines information transmission with energy transfer. As such, this feature offers a chance, particularly for the smaller gadgets (whose on-board energy is usually limited).

With SWIPT, wireless devices can do information processing and harvest energy from RF signals simultaneously. For SWIPT realization, two schemes are present: power splitting (PS) and time switching (TS). While in power splitting based SWIPT method, part of the power that is received is used for IP operations and the rest is utilized for energy harvesting (EH), TS-based SWIPT alternates the time between the IP and EH phases.

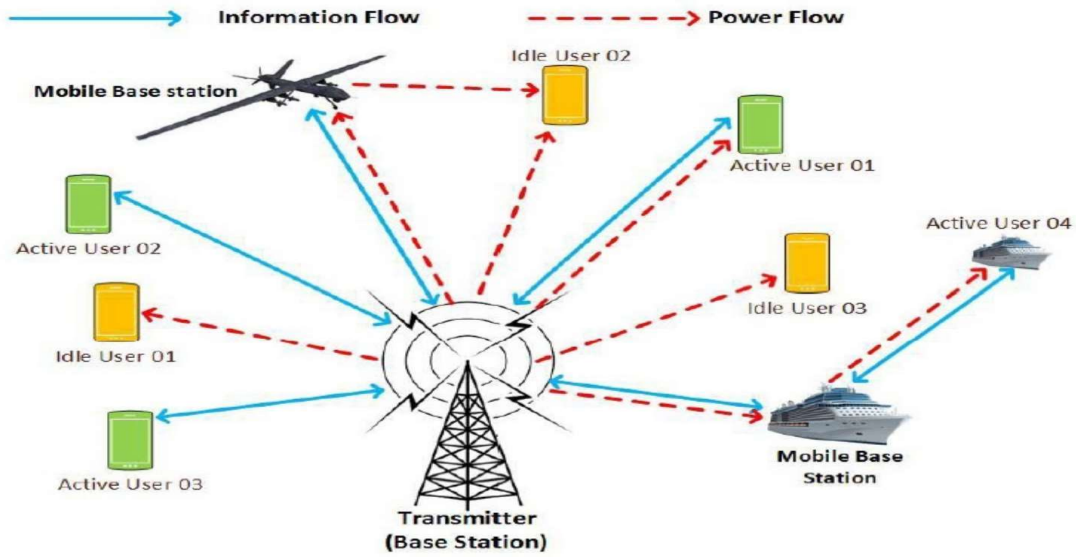


Figure 4: SWIPT via Static and Mobile Base Stations

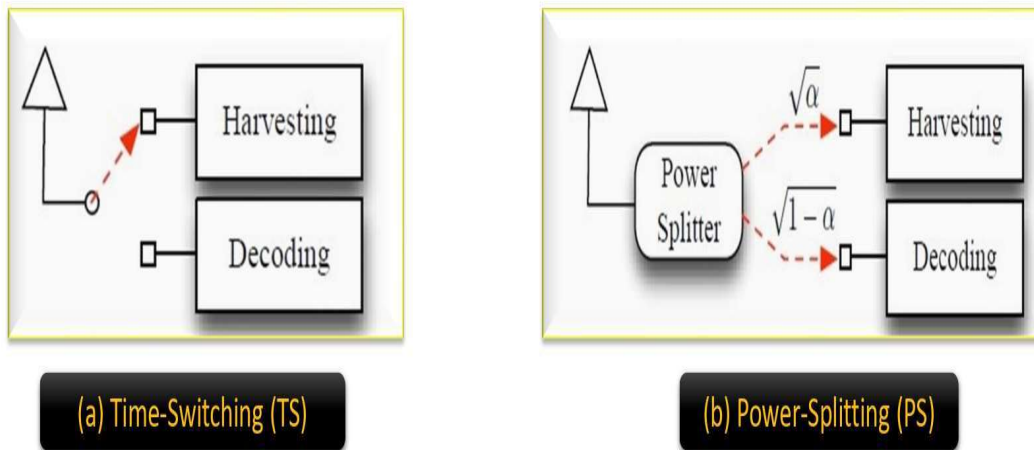


Figure 5: SWIPT Transmission Technique in Different Domains

## Chapter 4

### HALF-DUPLEX OVERLAY COGNITIVE SYSTEMS

For proper understanding of full duplex overlay cognitive systems first we study the half duplex overlay cognitive systems. In this section we shall look the system model, mathematical expressions required to study the full duplex overlay systems, ceiling effects etc.

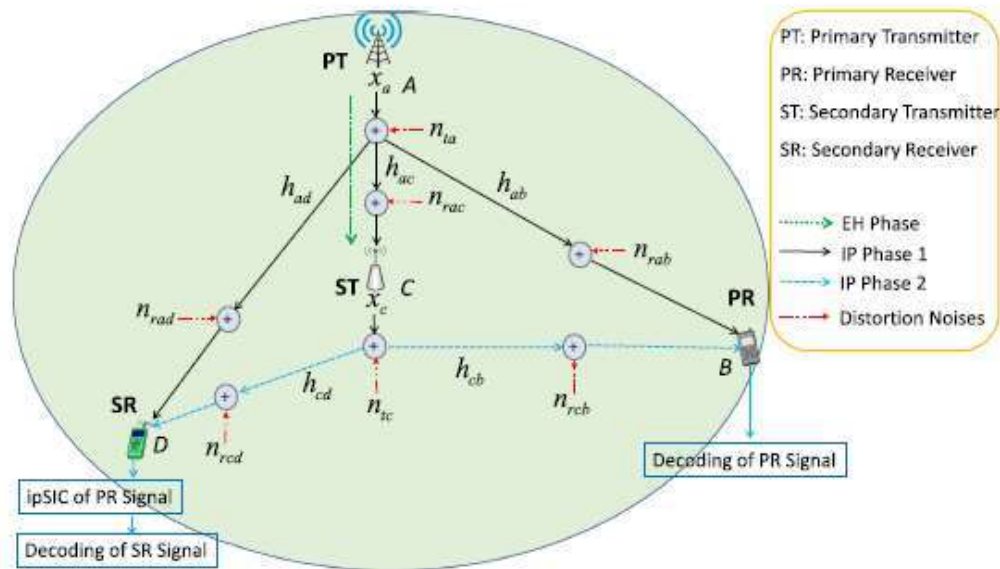


Figure 6: OCNOMA system model.

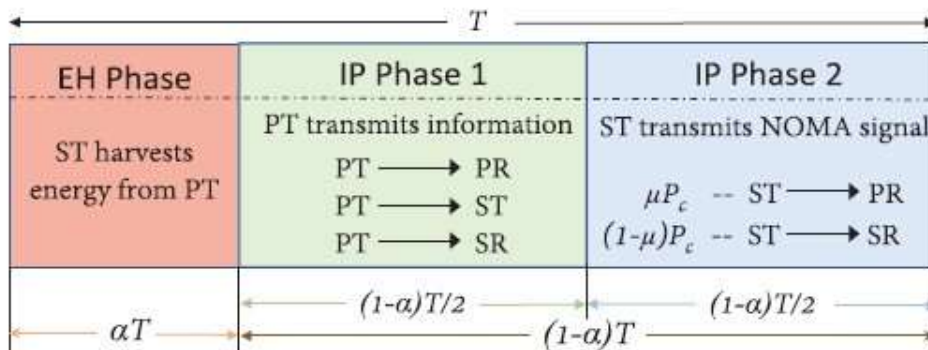


Figure 7: Block Structure of EH-based OCNOMA System for Transmission.

## 4.1 System Descriptions

### 4.1.1 System and Channel Models

We take into consideration above mentioned OCNOMA system that consists of a PT-PR pair coexisting with an ST-SR pair, as seen in Figure 6. Despite having a direct primary (DP) relationship with PR, the PT may nevertheless approach the neighbouring ST for assistance in order to take advantage of variety. As payment, the primary grants the ST access to its licensed spectrum for use in transmitting data to the SR. The PT sends the signal at a set transmit power and is thought to be fed by a steady power source. The PT transmits RF signals, from which energy is received by ST which is an energy-constrained node. Looking forward to cooperate with the primary transmission between PT and PR, ST is permitted to the licensed primary spectrum, based on an overlay paradigm. In order to accomplish this, using the NOMA technique and serving as a cooperative relay ST simultaneously transmits its signal to SR and assist in forwarding the PT's signal to PR. In this case, we choose a EH approach based on TS and investigate the underlying SSC scheme for the OCNOMA system under consideration through the use of DF relaying strategy, as detailed in the sequel.

We use the network nodes A, B, C, and D, respectively, to stand in for PT, PR, ST, and SR in the analytical framework. We take it for granted that every network node has a single antenna and runs in high definition. Moreover, devices have HIs since they are implanted with less expensive RF transceiver components. It is anticipated that all of the channels will follow the block fading, which will keep them constant for the duration of the block but allow them to alter on their own during the subsequent block transmission. For communication linkages between PT and PR, PT and ST, PT and SR, ST and PR, and ST and SR, the channel coefficients are represented and are subject to separate Nakagami- $m$  fading by  $h_{ab}$ ,  $h_{ac}$ ,  $h_{ad}$ ,  $h_{cb}$ , and  $h_{cd}$ , respectively.  $|h_{ij}|^2$ , the channel gain, is subjected to the Gamma distribution where  $\Omega_{ij}$  is the average power, and  $m_{ij}$ , the fading severity parameter, for  $i \in \{a, c\}$  and  $j \in \{b, c, d\}$ , with  $i \neq j$ . Therefore, expressions of PDF and CDF for the channel gain  $|h_{ij}|^2$  are

$$f_{|h_{ij}|^2}(x) = \left(\frac{m_{ij}}{\Omega_{ij}}\right)^{m_{ij}} \frac{x^{m_{ij}-1}}{\Gamma(m_{ij})} e^{-\frac{m_{ij}x}{\Omega_{ij}}} \quad (4.1)$$

and

$$F_{|h_{ij}|^2}(x) = \frac{1}{\Gamma(m_{ij})} \Upsilon\left(m_{ij}, \frac{m_{ij}}{\Omega_{ij}}x\right) \quad (4.2)$$

Regarding implementing the path loss model, we have  $\Omega_{ij} = d_{ij}^{-\nu}$ , where  $d_{ij}$  be the normalized distance between nodes  $i$  and  $j$ , and  $\nu$  is the path-loss exponent. In EH system based on the RF, It is must to extract RF energy at very low power density since the propagation energy drops off at the rate of  $d_{ij}^{-\nu}$ . Moreover, AWGN with variation  $\sigma^2$  and mean zero affects all receiving nodes. As depicted in Figure 7, the transmission block duration is split into three sub-blocks with the time splitting based EH model. The very first sub-block of time  $\alpha T$  is used for EH, and the remaining time  $(1 - \alpha)T$ , where  $\alpha \in (0, 1)$  is the TS parameter, is used for IP. The IP phase is further separated into two IP phases, each with a period of  $(1 - \alpha)T/2$ , because the nodes function in HD fashion. While ST uses the gathered power to send the NOMA signal to nodes PR, SR in the second IP phase, PT sends its own information to these nodes in the first IP phase.

### 4.1.2 EH Phase

The ST transmits the NOMA signal in the second IP phase after harvesting energy from the RF signal transmitted by the PT during the EH phase. Therefore, for a time of  $\alpha T$ , the captured energy at ST is given by

$$E_c = \Theta P_a |h_{ac}|^2 \alpha T \quad (4.3)$$

where  $P_a$  is the PT transmit power and  $\Theta$  is the energy conversion factor, which depends on the rectification procedure and related EH circuitry and varies from 0 to 1. Consequently, one can quantify the transmit power of ST across the interval  $(1 - \alpha)T/2$  as

$$P_c = \frac{E_c}{(1-\alpha)T/2} = \frac{2\Theta\alpha P_a |h_{ac}|^2}{1-\alpha} = \beta P_a |h_{ac}|^2 \quad (4.4)$$

Where  $\beta = \frac{2\Theta\alpha}{1-\alpha}$ . After EH phase, overall communication in proposed OCNOMA system happens in the two IP phases as described in the following subsections.

### 4.1.3 IP Phase

In initial IP phase, Information signal  $x_a$ , with  $E[|x_a|^2] = 1$ , is being transmitted to PR by PT

which is also received by the secondary nodes ST and SR. Therefore, the received signals  $y_{ab}, y_{ac},$  and  $y_{ad},$  at nodes  $B, C,$  and  $D,$  respectively, are given as

$$y_{ai} = h_{ai}(\sqrt{P_a}x_a + n_{ta}) + n_{rai} + v_{ai} \quad (4.5)$$

where  $i \in \{b, c, d\},$   $P_a$  is the transmitted power at  $A,$   $n_{ta} \sim \text{CN}(0, \lambda^2 P_a)$  shows the distortion noise, at node  $A,$  for transmit processing,  $n_{rai} \sim \text{CN}(0, \lambda^2 P_a |h_{ai}|^2)$  represents the distortion noise at  $i$ th node,  $\lambda_{ta}$  and  $\lambda_{rai}$  are the level of impairments, and  $v_{ai}$  is AWGN variable. hence, the resultant SNDR, through the DP link, at the  $i$ th node, where  $i \in \{b, c, d\}$  is given as

$$\Lambda_{ai}^{DP} = \frac{\Lambda_{ai}}{\Lambda_{ai}\lambda_{ai}^2 + 1} \quad (4.6)$$

Where  $\Lambda_{ai} = \eta_a |h_{ai}|^2$  with  $\eta_a = P_a / \sigma^2$  is the transmit SNR at node  $A,$  and  $\lambda_{ai} = \sqrt{\lambda_{ta}^2 + \lambda_{rai}^2}.$

The expressions for SINDR at the PR and SR are obtained by combining NOMA transmission at ST with DF-based relaying techniques, as we will discuss below.

#### 4.1.4 DF Relaying Strategy

Here, in the second IP phase, ST decodes the main signal  $x_a$  while including a DF-based relaying method. In the event that ST get success in decoding, to combine the decoded signal  $x_a$  to its own signal  $x_c,$  it applies the NOMA technique to generate a superimposed signal  $Z_c^{DF}.$  As a result, the ST node's signal is given by

$$Z_c^{DF} = \sqrt{\mu P_c} x_a + \sqrt{(1 - \mu) P_c} x_c + n_{tc} \quad (4.7)$$

The corresponding acquired signals at PR and SR from ST can then be obtained using  $y_{cb}^{DF}$  and  $y_{cd}^{DF},$  which are represented as

$$y_{cj}^{DF} = h_{cj} Z_c^{DF} + n_{rcj} + v_{cj} \quad (4.8)$$

As a result, using (7) and (8), the SNDR expression at PR can be stated as

$$\Lambda_{cb}^{DF} = \frac{\mu\beta\Lambda_{ac}|h_{cb}|^2}{\beta\Lambda_{ac}|h_{cb}|^2\rho_P+1} \quad (4.9)$$

the PR now uses MRC to combine the PT's signal components received in the first IP phase (via DP transmission) and second IP phase (via relay transmission), contingent on the PT's signal successfully decoding at ST.

On the other hand, the SR uses the NOMA concept to carry out SIC. In order to do this, the SR decodes the signal  $x_a$  from the PT first, takes  $x_a$  out of  $\mathcal{Y}_{cd}^{DF}$ , and then decodes its own signal,  $x_c$ . Prior to classifying ST's output as noise, the SR decodes the PT signal. Based on (4.7) and (4.8), the resulting SINDR expression at SR can therefore be stated as

$$\Lambda_{cd \rightarrow x_a}^{DF} = \frac{\mu\beta\Lambda_{ac}|h_{cd}|^2}{\beta\Lambda_{ac}|h_{cd}|^2\rho_S+1} \quad (4.10)$$

SR may now use the MRC to decode  $x_a$  in the SIC process because, as we remember, it heard the PT's signal during the initial IP phase. After that, SR is able to decode  $x_a$  and extract it from the NOMA signal  $\mathcal{Y}_{cd}^{DF}$ , that was received. The SINDR at SR, taking into account the I-SIC situation, can be written as

$$\Lambda_{cd}^{DF} = \frac{(1-\mu)\beta\Lambda_{ac}|h_{cd}|^2}{\beta\Lambda_{ac}|h_{cd}|^2\lambda_{cd}^2 + \zeta\mu\beta\Lambda_{ac}|h_D|^2 + 1} \quad (4.11)$$

where  $\rho_P = (1-\mu)\lambda_{cb}^2$  with  $\lambda_{cb} = \sqrt{\lambda_{tc}^2 + \lambda_{rcb}^2}$  and  $\rho_S = (1-\mu)\lambda_{cd}^2$  with  $\lambda_{cd} = \sqrt{\lambda_{tc}^2 + \lambda_{rcd}^2}$ .

In contrast, the signal  $x_a$  remains silent throughout the second IP phase if decoding of the signal is unsuccessful at ST in the first IP phase. In this instance, PR only receives  $x_a$  in the first IP phase from the PT via the DP link.

## 4.2 Performance Analysis of Primary Network

This segment examines the OP performance of the primary network with the DPT and SSC (with and without a DF relaying method) transmission systems. In line with this, we disclose significant ceiling effects related to the HIs, specifically the DPT ceiling and the SSC ceiling. Additionally, we look at determining the NOMA power allocation parameter's effective value extraction.

### 4.2.1 DPT Scheme

With no interaction from SSC, we therefore assume that DPT exclusively delivers communication via DP transmission. In order to compare the performance of the suggested SSC plan with this scheme, we investigate it first. OP of primary network utilizing DPT scheme for pre-defined goal rate  $R_p$  can be provided by, taking into account that DPT occurs during a single transmission phase

$$\mathcal{P}_{Pri}^{DP}(R_p) = Pr[\Lambda_{ai}^{DP} < Y_p'] = F_{\Lambda_{ab}^{DP}}(Y_p') \quad (4.12)$$

where,  $Y_p' = 2^{R_p} - 1$ . The CDF used in above equation can be represented by

$$F_{\Lambda_{ab}^{DP}}(Y_p') = Pr[\Lambda_{ab} < \frac{Y_p'}{1 - Y_p' \lambda_{ab}^2}] \quad (4.13)$$

which can be calculated, with the threshold condition  $Y_p'$ , as

$$\begin{aligned} F_{\Lambda_{ab}^{DP}}(Y_p') &= F_{\Lambda_{ab}}\left(\frac{Y_p'}{1 - Y_p' \lambda_{ab}^2}\right), \text{ if } Y_p' < 1 / \lambda_{ab}^2 \\ &= 1, \text{ if } Y_p' > 1 / \lambda_{ab}^2 \end{aligned} \quad (4.14)$$

Applying variable  $\Lambda_{ab} = \eta_a |h_{ab}|^2$  into (4.14), the needed OP can be computed. It is Observed, from (4.14), that when the threshold  $\gamma'p$  surpasses the value  $1/\lambda_{ab}^2$ , DPT persuades into outage. This is DPT ceiling effect due to HIs.

### 4.2.2 SSC Scheme

In this section, we analyse the OP performance for the proposed SSC scheme using DF relaying

for OCNOMA system as discussed in previous sections.

### SSC with DF Relaying (SSC-DF)

Considering the target rate  $R_p$ , the OP formulation for the primary network under SSC-DF is given by

$$\mathcal{P}_{Pri}^{DF}(R_p) = Pr[(\Lambda_{ab}^{DP} + \Lambda_{cb}^{DF}) < Y_p] (1 - F_{\Lambda_{ab}^{DP}}(Y_p)) + F_{\Lambda_{ab}^{DP}}(Y_p) F_{\Lambda_{ac}^{DF}}(Y_p) \quad (4.15)$$

$$\text{Where } Pr[(\Lambda_{ab}^{DP} + \Lambda_{cb}^{DF}) < Y_p] = \mathcal{P}_1$$

To compute (4.15), we evaluate the CDF  $F_{\Lambda_{ac}^{DF}}(Y_p)$  and probability  $\mathcal{P}_1$ . The CDF  $F_{\Lambda_{ac}^{DF}}(Y_p)$  is obtained by using

$$\begin{aligned} F_{\Lambda_{ac}^{DF}}(Y_p) &= F_{\Lambda_{ac}}\left(\frac{Y_p}{1 - Y_p \lambda_{ac}^2}\right), \text{ if } Y_p < 1/\lambda_{ac}^2 \\ &= 1, \text{ if } Y_p > 1/\lambda_{ac}^2 \end{aligned} \quad (4.16)$$

where  $\Lambda_{ac} = \eta_a |h_{ac}|^2$  the computation of  $\mathcal{P}_1$  can be done by

$$\mathcal{P}_1 = \int_0^{Y_p} \int_0^{Y_p - y} f_{\Lambda_{cb}^{DF}}(x) f_{\Lambda_{ab}^{DP}}(y) dx dy \quad (4.17)$$

With the help of above equations  $\mathcal{P}_{Pri}^{DF}(R_p)$  can be evaluated.

### 4.2.3 Ceiling Effects

The ceiling effects are of two types, known as RCC and DPC, may be more likely to occur in an SSC scheme when HIs are present. In an OCNOMA system, the RCC effect happens when undesirable limitations placed on the threshold  $Y_p$  cause relay cooperation to fail an example of RCC is the SSC DF system. Herein, relay cooperation ceases and the OP of the primary network anticipates on the DPT only when  $Y_p$  reaches the value  $\mu/\rho_p$  for SSC-DF relaying. Furthermore, when  $Y_p$  rises above  $1/\max(\lambda_{ab}^2, \lambda_{ac}^2)$ , for the SSC-DF example, the primary transmission experiences an outage, which is ascribed to DPC. Keep in mind that the calculated value of  $\mu/\rho_p$  is always less than  $1/\max(\lambda_{ab}^2, \lambda_{ac}^2)$ , for the practical ranges of  $\mu$ , meaning that RCC always emerges before DPC. In order to design a workable OCNOMA system, one can

determine a reasonable limit on HIs level with a goal data rate based on the aforementioned statements.

### 4.3 Performance Analysis of Secondary Network

In this part, the two SIC cases I-SIC and P-SIC as well as the OP analysis of the secondary network under the SSC-DF scheme are discussed. It also enhances the ceiling effects of the secondary network.

#### 4.3.1 SSC-DF Scheme

For a target rate of  $R_s$ , the OP calculation for the secondary network under the SSC-DF plan is shown as

$$\mathcal{P}_{Sec}^{DF}(R_s) = [(1 - F_{\Lambda_{ac}^{DP}}(\gamma_p))] F_{\Lambda_{cd}^{DF}}(\gamma_s) + F_{\Lambda_{ac}^{DP}}(\gamma_p) \quad (4.18)$$

To compute (4.18), we need the expression for  $F_{\Lambda_{cd}^{DF}}(\gamma_s)$  which is computed in the following subsections.

#### I-SIC

The expression of  $F_{\Lambda_{cd}^{DF}}(\gamma_s)$  for the case of I-SIC is provided by the following theorem

$$\begin{aligned} F_{\Lambda_{cd}^{DF}}(\gamma_s) &= \psi_4(\gamma_s) - \psi_5(\gamma_s), & \text{if } (\gamma_s) < (1 - \mu)/\lambda_{cd}^2 \\ &= 1, & \text{if } (\gamma_s) \geq (1 - \mu)/\lambda_{cd}^2 \end{aligned} \quad (4.19)$$

#### P-SIC

In this instance, the secondary network's output power under the SSC-DF scheme can be calculated using  $F_{\Lambda_{cd}^{DF}}(\gamma_s)$  which is provided as

$$\begin{aligned} F_{\Lambda_{cd}^{DF}}(\gamma_s) &= \psi_6(\gamma_s), & \text{if } (\gamma_s) < (1 - \mu)/\lambda_{cd}^2 \\ &= 1, & \text{if } (\gamma_s) \geq (1 - \mu)/\lambda_{cd}^2 \end{aligned} \quad (4.20)$$

Where  $\psi_4$ ,  $\psi_5$  and  $\psi_6$  are constraints which can be calculated .

### 4.3.2 Ceiling Effects

When restrictions on the threshold  $\gamma_s$  prevent ST from transmitting data to its destination SR, the secondary network experiences the ceiling effect. This could be realised for the P-SIC case from (4.20), when  $\gamma_s \geq (1-\mu)/\lambda_{cd}^2$  for SSC-DF scheme. Furthermore, the value of  $(1-\mu)/\lambda_{cd}^2$  is always less than  $1/\lambda_{ac}^2$  for the viable ranges of  $\mu$ , therefore,  $(1-\mu)/\lambda_{cd}^2$  shows an important role in deciding the threshold value for SSC-DF scheme. As a result, the relevant ceiling effect has an impact on the secondary communication and causes outage. Conversely, in the case of the I-SIC mode, the fading severity parameter and IS channel power gain cause the ceiling phenomena to manifest at a comparatively lower threshold  $\gamma_s$  for the SSC-DF scheme.

## 4.4 Overall OCNOMA System Performance

Building on the developments from earlier sections, we analyse the throughput and energy efficiency performance for the entire OCNOMA system in this section.

### 4.4.1 System Throughput

One noteworthy performance metric to evaluate the spectrum usage for the OCNOMA system under consideration is the system throughput. It essentially indicates the mean SE for wireless systems based on cooperative communication. It can be displayed as the sum of the separate primary and secondary communication target rates that are achievable over the Nakagami m fading channels for the proposed OCNOMA system. We can determine the system throughput for the corresponding SSC-DF scheme by using the obtained OP equations for the primary and secondary networks.

$$S_T^{DF} = \frac{(1-\alpha)}{2} [(1 - \mathcal{P}_{Pri}^{DF}(R_p))(R_p) + (1 - \mathcal{P}_{Sec}^{DF}(R_s))\mathcal{P}_{Sec}^{DF}(R_s)] \quad (4.21)$$

Observing that the maximum system throughput for the SSC scheme with  $R_p = R_s = R$  set is  $R(1-\alpha)$ , this might be achieved in a high SNR regime with perfect hardware and P-SIC conditions.

### 4.4.2 Energy Efficiency

We are able to analyse the energy efficiency of the EH-based OCNOMA system under the

SSCDF scheme by utilizing the throughput expression in (4.21). Such type of study can aid in the design of an EH based OCNOMA system to increase the lifetime of the network. In essence, the system's energy efficiency could be defined as the proportion of provided data to total energy used. For the SSC-DF scheme, the system throughput, as stated in (4.21), shows the whole amount of data supplied. On the other hand, with the TS-based EH method in the SSC scheme, the total energy used in the system is the product of the energy used by the PT during the EH phase (of time  $\alpha T$ ) and the energy used by it during the first IP phase (of duration  $(1 - \alpha)T/2$ ). It is important to remember that the energy used in the second IP phase is the same energy that ST gathered during the EH phase, thus it does not contribute to the system's overall energy consumption. Therefore, using the SSC-DF scheme, the energy efficiency of the OCNOMA system under consideration can be stated as

$$\mathcal{E}^{DF} = \frac{S_T^{DF}}{Pa \left[ \alpha + \frac{(1-\alpha)}{2} \right]} \quad (4.22)$$

where  $S_T^{DF}$  is in bps/Hz.

## Chapter 5

# FULL-DUPLEX OVERLAY COGNITIVE NOMA SYSTEMS

## 5.1 Description of Signal and System Models

First, we discuss the signal model related to HIs in this part. Next, we outline the system and channel models for the suggested network that is influenced by FD OCNOMA.

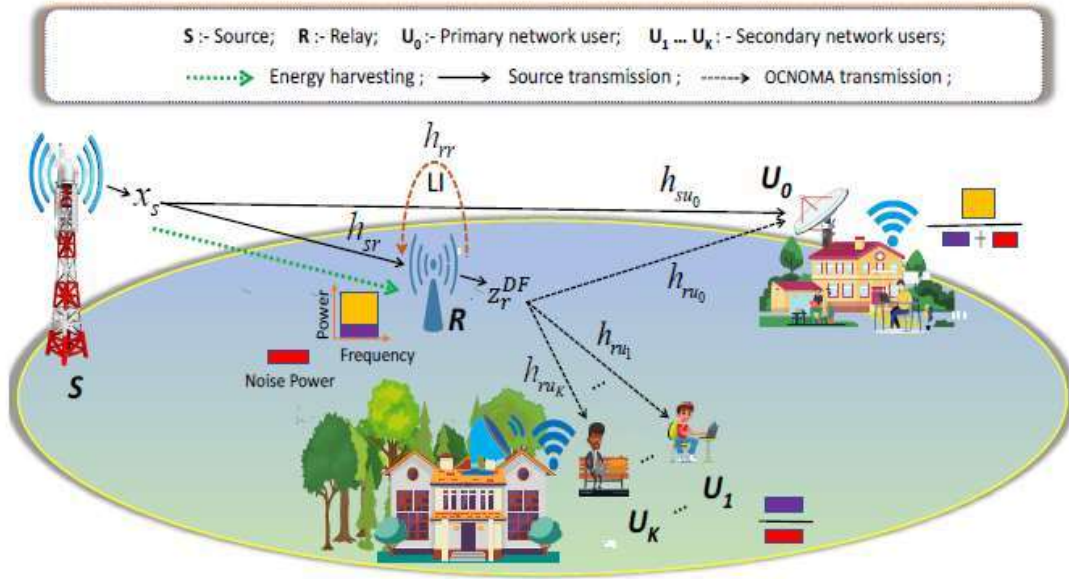


Figure 8: System Model for FD OCNOMA

### 5.1.1 Signal Model with Hardware Impaired Signal Model (HIs)

Let  $x_i$  be the signal to be communicated through a wireless fading channel, as shown in Fig. 7, and let  $h_{ij}$  be the coefficient of the fading channel between any two random nodes,  $i$  and  $j$ . As a result, the signal received at the  $j$ th node can be expressed conventionally (without HIs) as

$$y_j = h_{ij}x_i + \psi_j \quad (5.1)$$

where  $\psi_j$  is the AWGN (additive white Gaussian noise) variable, labelled as  $\psi_j \sim CN(0, \sigma^2)$  with the HIs in the model, given as

$$\mathcal{Y}_j = h_{ij}(x_i + n_{ti}) + n_{rij} + \psi_j \quad (5.2)$$

where  $n_{ti} \sim CN(0, \theta_{ti}^2 P_i)$  is distortion noise at transmitter section and  $n_{rij} \sim CN(0, \theta_{rij}^2 P_i |h_{ij}|^2)$  is distortion noise at receiver section.  $P_i$  being the power at  $i$ th node where  $P_i = E[|x_i|^2]$ ,  $\theta_{ti}$  and  $\theta_{rij}$  are the level of impairments which the experimenter can quantify as the error vector magnitude (EVMs). Due to accumulated distortion noises, the total power at the receiver is expressed as

$$E[|h_{ij}n_{ti} + n_{rij}|^2] = P_i |h_{ij}|^2 (\theta_{ti}^2 + \theta_{rij}^2) = P_i |h_{ij}|^2 \theta_{ij}^2 \quad (5.3)$$

With  $\theta_{ij}^2 = \theta_{ti}^2 + \theta_{rij}^2$  is the receiving nodes' corresponding HI. By using (5.3), (5.2) can be expressed as

$$\mathcal{Y}_j = h_{ij}(x_i + n_{ij}) + \psi_j \quad (5.4)$$

where  $n_{ij} \sim CN(0, \theta_{ij}^2 P_i)$  is equivalent distortion noise at the receiving nodes. Additionally, we presume that the hardware on each node is of the same calibre. If every node has perfect hardware, then  $\theta_{ij} = 0$ . We will use (5.4) to record the effects of HIs while safeguarding the main features of the channel for further investigation.

### 5.1.2 System Model

We assume an FD OCNOMA inspired network, as depicted in Fig. 8, consists of a main source ( $S$ )–user ( $U_0$ ) pair coexisting with a secondary source  $R$  and its  $K$  intended users  $U_k$ , which can be any number from 1 to  $K$ . Despite having a direct transmission (DT)-link with its user  $U$ , primary source  $S$  uses node  $R$  to assist in establishing a CSST-link in order to take advantage of diversity. In this way,  $R$  serves as a cooperative DF relay for primary communication and obtains primary spectrum access in exchange for the ability to transmit data directly to users  $\{U_k\}_{k=1}^k$ . Because node  $S$  is regarded as a power rich node, it transmits data to user  $U_0$  using a continuous power source. On the other hand, node  $R$ , the node with limited power, gathers energy from the RF signal that node  $S$  transmits.  $R$  employs the NOMA principle to broadcast its individual data to users  $\{U_k\}_{k=1}^k$  and to relay the primary source data to user  $U_0$ , based on the overlay spectrum sharing model. Furthermore,  $R$  uses two different antennas to do

simultaneous reception and transmission in order to support the FD mode of operation; in contrast, all other nodes in Fig. 8 use a single antenna. Despite the fact that a number of strategies have been put forth to lessen the LI impacts in FD systems, LI still affects the relay node and is strongly correlated with the transmit power utilized at the FD relay node. It is believed that the SUs  $\{U_k\}_{k=1}^k$  are obscured from the source S by shadowing or other obstacles.

### 5.1.3 Channel Model

Every channel is assumed to experience block fading, in which case it stays the same for the current block transmission but could vary for the subsequent block transmission. We use  $h_{su_0}$ ,  $h_{sr}$ ,  $h_{sr}$ ,  $h_{ruk}$ , and  $h_{rr}$ , to denote the coefficient of the channel between  $S \rightarrow U_0$ ,  $S \rightarrow R$ ,  $R \rightarrow U_0$ ,  $R \rightarrow U_k$ , and  $R \rightarrow R$ , respectively. We additionally take into account that the channel coefficients  $h_{ij}$ ,  $i \in \{s, r\}$ ,  $j \in \{u_0, r, u_k\}$ , and  $k \in \{1, \dots, K\}$ , adhere to separate Nakagami-m distributions. We assume that the average LI power  $E[|h_{rr}|^2] = \Omega_{rr}$  for the LI fading channel coefficient  $h_{rr}$ , which follows Nakagami-m fading. On the other hand, since  $E[|h_{rr}|^2]$  is relatively tiny because self-interference suppression is of good quality in practice, we can replace  $|h_{rr}|^2$  by  $\Omega_{rr}$ .

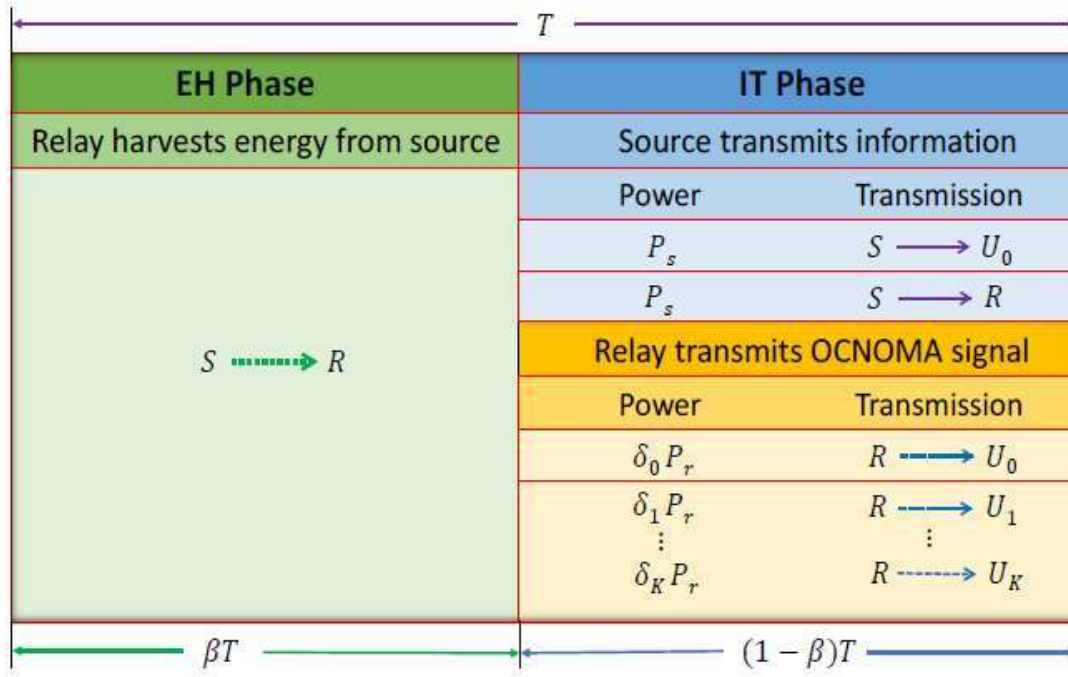


Figure 9: Transmission block using TS-based EH protocol for the FD OCNOMA system

## 5.2 Description of CSST Scheme

This subsection describes FD based CSST techniques for SWIPT in the studied OCNOMA system for both TS as well as PS protocols.

According to the sequel, entire transmission process under the CSST scheme occurs in a single transmission block of length  $T$ , combining DF-relaying with OCNOMA transmission from the secondary source and SWIPT with main source transmission.

### 5.2.1 SWIPT with Primary Source Transmission

#### TS based EH Protocol

In this case, energy is harvested from the primary source  $S$  by relay node  $R$  using an EH protocol based on TS. Fig. 9 illustrates the transmission block architecture for the FD OCNOMA system for this protocol. It is separated into two time slots. Relay gathers energy from the Radio Frequency signal broadcast by source  $S$  during the first time slot, which has a period of  $\beta T$ . Meanwhile, IT uses the second time slot, which has a period of  $(1 - \beta)T$ , where  $\beta$  is the TS parameter and  $\in (0, 1)$ . Relay absorbs energy from the primary source signal, just like it did in the first time slot, and uses it to transmit the OCNOMA signal during the IT phase. The gathered energy, therefore for duration  $\beta T$  is given by

$$E_{r,TS} = \eta |h_{sr}|^2 P_s \beta T \quad (5.5)$$

here  $P_s$  is transmitting power at source  $S$ , and  $\eta$  be the energy conversion factor, depending on the EH circuit and the rectification process, such that  $0 < \eta < 1$ . As a result, we assumed that node  $R$ 's power harvesting varied linearly with energy. It should be noted that while energy collected from AWGN or hardware generated distortion noise is substantially less than that from the source's transmitted RF signal, it is ignored. Furthermore, the energy collected at the relay is ignored in the event of circuit consumption and is solely utilized to power the IT for end users  $U_0, \dots, U_k$ . The information is then transmitted by the relay with power  $P_{r,TS}$  for a period of  $(1 - \beta)T$ , as indicated by

$$P_{r,TS} = \frac{E_{r,TS}}{(1 - \beta)T} = \frac{\eta |h_{sr}|^2 P_s \beta T}{(1 - \beta)T} = \zeta_{TS} |h_{sr}|^2 P_s \quad (5.6)$$

where  $\zeta_{TS} = \frac{\eta \beta T}{(1 - \beta)T}$ . When operating in the FD relaying mode, which is detailed in the sequel, all communication proposed in the OCNOMA system occurs in a single IT phase following the EH phase.

Source  $S$  delivers the information signal  $x_0(t)$ , to  $U_0$  during the IT phase, complying  $E[|x_0(t)|^2] = 1$ , It is additionally picked up by the secondary node  $R$ . As a result,  $y_{su_0}(t)$  and  $y_{sr}(t)$ , respectively, reflect the received signals at nodes  $U_0$  and  $R$ . Consequently, at the  $t$ th time instant, the signals received by user  $U_l$  over the DT-link can be expressed as

$$y_{su_0}(t) = h_{su_0}(\sqrt{P_s}x_0(t) + n_{su_0}(t)) + \psi_{su_0}(t) \quad (5.7)$$

where  $n_{su_0}(t) \sim CN(0, \theta_{su_0}^2 P_s)$  is distortion noise at node  $U_0$ , with  $\theta_{su_0}^2 = \theta_{ts}^2 + \theta_{rsu_0}^2$ ,  $\theta_{ts}$  and  $\theta_{rsu_0}$  are the level of hardware impairments, and  $\psi_{su_0}(t)$  be the AWGN variable. As a result, the final SNDR, via the DT-link, at node  $U_0$  can be acquired as

$$\gamma_{su_0}^{DT} = \frac{|h_{su_0}|^2 P_s}{|h_{su_0}|^2 P_s \theta_{su_0}^2 + \sigma^2} = \frac{\gamma_{su_0}}{\gamma_{su_0} \theta_{su_0}^2 + 1} \quad (5.8)$$

where  $\gamma_{su_0}$  is the transmit SNR at node S.

## PS-based EH Protocol

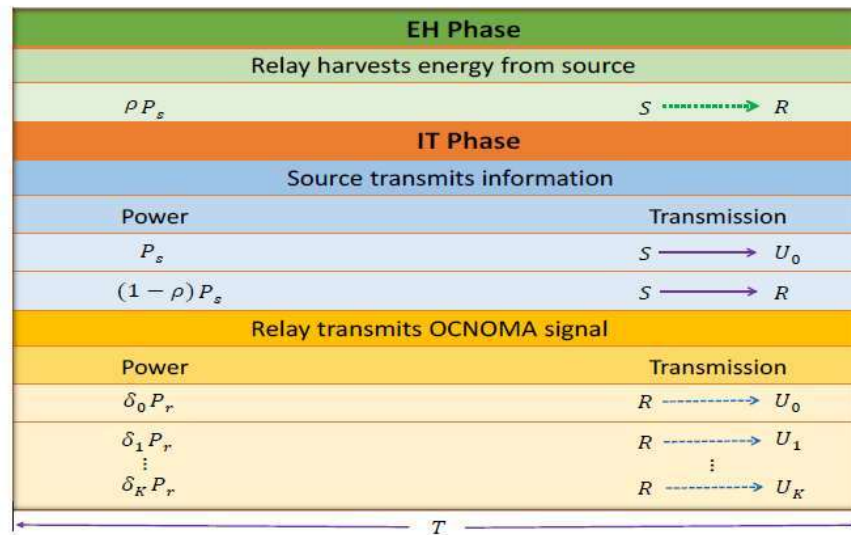


Figure 10: Transmission block with PS-based EH protocol for the FD OCNOMA system

For the FD OCNOMA system, the block transmission time is shown in Figure 10 using the PS-based EH protocol. In this case, EH uses a fraction  $\rho$  ( $0 < \rho < 1$ ) of the received radio frequency signal power from source  $S$ , whereas information decoding uses the remaining fraction  $(1 - \rho)$ . As a result, the energy collected at  $R$  can be given as

$$E_{r,PS} = \eta\rho(|h_{sr}|^2P_s + P_{r,PS}|h_{rr}|^2)T \quad (5.9)$$

here  $P_{r,PS}$  is the relay  $R$ 's transmit power and  $0 < \eta < 1$  denotes the energy conversion efficiency. It should be noted that the FD relay node  $R$  uses the LI channel to obtain its own energy as well as the dedicated energy from the source  $S$ . Node  $R$  uses the energy that has been gathered to power the IT. Consequently,  $R$ 's transmit power is determined by

$$P_{r,PS} = \frac{\eta\rho|h_{sr}|^2P_s}{1-\eta\rho|h_{rr}|^2} = \zeta_{PS}|h_{sr}|^2P_s \quad (5.10)$$

where  $\zeta_{PS} = \frac{\eta\rho}{1-\eta\rho|h_{rr}|^2}$ .

and the modelled signal at  $R$  is given as

$$\begin{aligned} y_{sr,PS}(t) = & (\sqrt{(1-\rho)P_s}h_{sr}x_0(t)) + (\sqrt{(1-\rho)P_s}h_{sr}n_{sr}(t)) + \\ & \sqrt{(1-\rho)h_{rr}}(\sqrt{P_{r,PS}}x_r(t-\tau) + n_{rr}(t-\tau)) + \sqrt{(1-\rho)}\psi_{sr}(t) + \psi_{o,r}(t) \end{aligned} \quad (5.11)$$

where the sampled AWGN due to RF to baseband signal conversion is shown by  $\psi_{o,r}(t)$ . We disregard the antenna noise,  $\psi_{sr}(t)$ , in the following study since its strength is substantially lower than the circuit processing noise,  $\psi_{o,r}(t)$ . Thus, using the DT-link, the final SNDR at node  $R$  can be expressed as

$$\gamma_{sr,PS}^{DT} = \frac{(1-\rho)\gamma_{sr}}{(1-\rho)\zeta_{PS}|h_{rr}|^2(1+\theta_{rr}^2)\gamma_{sr} + (1-\rho)\theta_{sr}^2\gamma_{sr} + 1} \quad (5.12)$$

The DF relaying with OCNOMA transmission for both the TS as well as PS protocols is described here, and as a result, the matching SINDR expressions at the users  $U_0$  and  $\{U_k\}_{k=1}^K$  are obtained.

## 5.2.2 DF-Relaying with OCNOMA Transmission

By using the relay link, the SINDR at  $U_0$  is expressed as

$$\gamma_{ru_0, \ell}^{DF} = \frac{\delta_0 \zeta_\ell \gamma_{sr} |h_{ru_0}|^2}{\delta_0 \zeta_\ell \gamma_{sr} |h_{ru_0}|^2 (\sum_{i=1}^K \delta_i + \theta_{ru_0}^2) + 1} \quad (5.13)$$

where  $\zeta_\ell$  be the factor defined for the TS and PS protocols.

## 5.3 Performance Analysis of Primary Network

Applying the FD based CSST scheme revealed in the aforesaid part, we analyse the OP performance of the primary network for the OCNOMA system under consideration in this part. Additionally, we provide OP analysis for main network using DPT alone method in order to compare performance and determine the efficacy of spectrum sharing. In turn, we uncover some significant ceiling effects related to the HIs. Additionally, we look into determining the effective value of power allocation parameter of FD OCNOMA extraction.

### 5.3.1 DPT Scheme

Here, we take it for granted that DPT only uses a DT-link to facilitate primary communication between  $S$  and  $U_0$ ; that is, there is no participation of spectrum sharing through relay cooperation with secondary node  $R$ . We examine this scheme in order to compare its performance with that of the suggested FD based CSST method. Given that the DPT method necessitates a single transmission phase, the OP of the primary network employing the DPT system can be determined by for a predetermined target rate  $r_{th}^p$ .

$$\mathcal{P}_{Pri}^{DT}(r_{th}^p) = Pr[\gamma_{su_0}^{DT} < \tau_p^{DT}] = F_{\gamma_{su_0}^{DT}}(\tau_p^{DT}) \quad (5.14)$$

where  $\tau_p^{DT} = 2^{r_{th}^p} - 1$  indicates the DT-link SNDR threshold. (5.8) can be used to represent the CDF in (5.14) as

$$F_{\gamma_{su_0}^{DT}}(\tau_p^{DT}) = Pr \left[ \gamma_{su_0} < \frac{\tau_p^{DT}}{1 - \theta_{su_0}^2 \tau_p^{DT}} \right] \quad (5.15)$$

and can be calculated using the threshold  $\tau_p^{DT}$  condition as

$$F_{\gamma_{su_0}^{DT}}(\tau_p^{DT}) = \begin{cases} F_{\gamma_{su_0}}\left(\frac{\tau_p^{DT}}{1 - \theta_{su_0}^2 \tau_p^{DT}}\right), & \text{if } \tau_p^{DT} < \frac{1}{\theta_{su_0}^2} \\ = 1 & \text{if } \tau_p^{DT} \geq \frac{1}{\theta_{su_0}^2} \end{cases} \quad (5.16)$$

### 5.3.2 CSST Scheme

As mentioned in Section 5.2, we now evaluate the OP performance for FD-based CSST scheme for main network. The formulation of OP for the primary network under CSST scheme can be obtained by taking the target rate,  $r_{th}^p$ , into consideration

$$\mathbb{P}_{Pr,i,\ell}^{CSST}(r_{th}^p) = \mathbb{P}_{u_0,\ell} + F_{\gamma_{sr,\ell}^{DT}}(\tau_{p,\ell}) F_{\gamma_{su_0}^{DT}}(\tau_{p,\ell}) \quad (5.17)$$

To compute (5.17), we evaluate CDFs  $F_{\gamma_{sr,\ell}^{DT}}(\tau_{p,\ell})$ ,  $F_{\gamma_{su_0}^{DT}}(\tau_{p,\ell})$ , probability term  $\mathbb{P}_{u_0,\ell}$ . We also obtained the expressions for the CDF  $F_{\gamma_{su_0}^{DT}}(\tau_{p,\ell})$  from (5.16). To calculate the CDF  $F_{\gamma_{sr,\ell}^{DT}}(\tau_{p,\ell})$  is represented as

$$\gamma_{sr,\ell}^{DT} = \frac{\xi_\ell \gamma_{sr}}{\xi_\ell \zeta_\ell \gamma_{sr} |h_{rr}|^2 (1 - \theta_{rr}^2) + \xi_\ell \gamma_{sr} \theta_{sr}^2 + 1} \quad (5.18)$$

where  $\xi_{TS} = 1$  and  $\xi_{PS} = 1 - \rho$  are protocols for TS and PS, respectively. Therefore, the CDF  $F_{\gamma_{sr,\ell}^{DT}}(\tau_{p,\ell})$  with threshold  $\tau_{p,\ell}$ , condition can be calculated from equation given below

$$F_{\gamma_{sr,\ell}^{DT}}(\tau_{p,\ell}) = \begin{cases} F_{|h_{sr}|^2}\left(\frac{\mu_\ell}{\Delta_s}\right), & \text{if } \tau_{p,\ell} < \frac{1}{\phi_\ell} \\ = 1 & \text{if } \tau_{p,\ell} \geq \frac{1}{\phi_\ell} \end{cases} \quad (5.19)$$

where  $\mu_\ell = \frac{\tau_{p,\ell}}{\xi_\ell (1 - \tau_{p,\ell}) \Phi_\ell}$  with  $\phi_\ell = \zeta_\ell \Omega_{rr} (1 + \theta_{rr}^2) + \theta_{sr}^2$ . Hereby, applying (4.2) for CDF of  $|h_{sr}|^2$  into (5.19), the needed CDF of  $\gamma_{sr,\ell}^{DT}$  can be obtained. Observing from (5.19), the DT over S-R connection convinces itself to go down as the threshold  $\tau_{p,\ell}$  approaches  $\frac{1}{\phi_\ell}$ . This is explained as the result of the DT ceiling effect brought on by the HIs and LI.

### 5.3.3 Ceiling Effects in CSST

The CSST scheme applied for the FD OCNOMA system may be predisposed to the FRC and ESC ceiling effects due to the presence of HIs. When undesired constraints are placed on the threshold  $\tau_{p,\ell}$ , relay cooperation in the FD OCNOMA system experiences an outage. This is when the FRC effect takes place. It is obvious from (5.19) that,  $\tau_{p,\ell} \geq \frac{1}{\zeta\ell\Omega r r(1+\theta_{rr}^2) + \theta_{sr}^2}$ , the CDF  $F_{\gamma_{sr,\ell}^{DT}}(\tau_{p,\ell})$  attains unity, causing halts in the relay cooperation. As a result, the OP performance of primary network only predicts the DT-link. Further, depending on DT in (5.16) and (5.17), the DT also experiences an outage that is ascribed to ESC as  $\tau_{p,\ell}$  gets closer to the value  $\frac{1}{\theta_{su_0}^2}$ . Keeping in mind that the numerical value of is always less than  $\frac{1}{\theta_{su_0}^2}$  or  $\frac{1}{\zeta\ell\Omega r r(1+\theta_{rr}^2) + \theta_{sr}^2}$ , which means that FRC always comes before ESC and that  $\tau_{p,\ell}$  is what determines relay cooperation to primary communication for the attainable ranges of power allocation parameter and other system parameters. The aforementioned statements can be used to calculate a workable limit on hardware impairments level and a goal data rate for designing an effective FD OCNOMA system.

## 5.4 Performance Analysis of Secondary Network

This subsection examines the OP performance for the secondary network of the OCNOMA system below the FD-based CSST scheme, taking into account the SIC cases—I-SIC and P-SIC. Moreover, it enhances the ceiling effects of the secondary network.

### 5.4.1 FD-based CSST Scheme

As long as the relay R is able to successfully decode  $x_0(t)$ , the user  $U_k$  is regarded to be in an outage. This also applies when the relay R is unable to decode any  $x_m(t)$ ,  $0 \leq m \leq k$ . For a target rate  $r_{th}^S$ , the OP of user  $U_k$  under the FD OCNOMA system can therefore be formulated as

$$P_{sec,u_k,\ell}^{CSST}(r_{th}^S) = Pr[\gamma_{sr,\ell}^{DT} < \tau_{p,\ell}] + Pr[\gamma_{sr,\ell}^{DT} \geq \tau_{p,\ell}, \dot{p}_{u_k,\ell}] \quad (5.20)$$

Where  $P_{u_k,\ell} = Pr[\gamma_{sr,\ell}^{DT} \geq \tau_{p,\ell}, \dot{p}_{u_k,\ell}]$  and  $\dot{p}_{u_k,\ell}$  is the OP which the user  $U_k$  unable to decode for any  $x_m(t)$ ,  $0 \leq m \leq k$ .

$\dot{p}_{u_k,\ell}$  is given as

$$\hat{p}_{u_k, \ell} = 1 - Pr [ \varepsilon_{u_k, x_0, \ell}^c \cap \dots \cap \varepsilon_{u_k, x_0, \ell}^c ] \quad (5.21)$$

Where  $\varepsilon_{u_k, x_m, \ell}^c = \{ \gamma_{r_{u_k, x_m, \ell}}^{DF} \geq \tau_{s, \ell} \}$ ,  $0 \leq m \leq k$ , is that event which user  $U_k$  abely decodes  $x_m$ , with  $\tau_{s, \ell} = 2^{k\ell r_{th}^s} - 1$ .

### P-SIC

Further (5.20) can be evaluated as

$$\mathbb{P}_{sec, u_k, \ell}^{CSST} (r_{th}^s) = P_{u_k, \ell} + F_{\gamma_{sr, \ell}^{DT}}(\tau_{p, \ell}) \quad (5.22)$$

### I-SIC

Further (5.20) can be evaluated as

$$\mathbb{P}_{sec, u_k, \ell}^{CSST} (r_{th}^s) = \left[ 1 - F_{\gamma_{sr, \ell}^{DT}}(\tau_{p, \ell}) \right] F_{\gamma_{ru_k, x_k, \ell}^{DF}}(\tau_{s, \ell}) + F_{\gamma_{sr, \ell}^{DT}}(\tau_{p, \ell}) \quad (5.23)$$

## 5.4.2 Ceiling Effects

The so-called SNC ceiling effect affects the secondary network. The SNC effect happens when restrictions placed on the threshold  $\tau_{s, \ell}$  prevent node  $R$  from transmitting data to its destination, the United Kingdom. This might be understood as the OP in (5.22) turns into oneness, leading to the breakdown of the secondary communication. Furthermore, across the viable parameter ranges, the numerical value is always less than  $\frac{1}{\phi_\ell}$ . Consequently, the optimal value of  $\tau_{s, \ell}$  is crucial in determining the secondary communication threshold. As a result, the relevant ceiling effect affects and experiences the secondary communication. Remarkably, for P-SIC, the SNC phenomena manifests at a comparatively higher threshold value  $\tau_{s, \ell}$  for the FD-based CSST scheme than for ISIC; consequently, the former facilitates a higher data rate for the secondary connection.

## 5.5 Overall FD OCNOMA System Performance

Depending on the studies in previous parts, we analyse the throughput and energy efficiency performance for the entire FD OCNOMA system in this section.

### 5.5.1 System Throughput

One necessary performance metric to evaluate the utilization of spectrum for the FD OCNOMA system under consideration is the system throughput. It essentially indicates the mean SE for wireless systems based on cooperative communication. It is represented as the sum of the individual target rates of primary and secondary transmissions that are achievable over the Nakagami-m fading channels for the proposed FD OCNOMA system. With the primary and secondary networks' derived OP expressions as a guide, the system throughput for the FD-based CSST scheme may be calculated as

$$\mathbb{S}_{T,\ell}^{CSST} = \frac{1}{K_\ell} [(1 - \mathbb{P}_{Pri,\ell}^{CSST}(r_{th}^p))r_{th}^p + \sum_{k=1}^K (1 - \mathbb{P}_{sec,u_k,\ell}^{CSST}(r_{th}^s))r_{th}^s] \quad (5.24)$$

From (5.24), We note that for the FD OCNOMA system under CSST scheme, the maximum feasible system throughput is  $(1 - \beta)(1 + K) R$ , which might be reached when the OP terms approach zero, with setting  $r_{th}^p = r_{th}^s = R$ .

### 5.5.2 Energy Efficiency

Here we analyse the energy efficiency for the proposed FD OCNOMA system by CSST scheme, making use of the throughput expression in (5.24). Such study can aid in the design of an EH-aware FD OCNOMA system to increase the lifetime of network. In essence, the system's energy efficiency is defined as the proportion of provided data to total energy used. For the FD based CSST method, the system throughput as stated in (5.24) is the total amount of data supplied. On the other hand, for both TS as well as PS based EH protocols, the total energy used in the system is the total energy used by source  $S$  throughout the whole block duration of  $T$ . It is important to remember that the energy used for relay transmission comes from  $R$ 's harvest, thus it doesn't add to the system's overall energy consumption. Therefore, using the CSST technique, the energy efficiency of the FD OCNOMA system can be stated as

$$\eta_{EE,\ell}^{CSST} = \frac{\mathbb{S}_{T,\ell}^{CSST}}{P_s} \quad (5.25)$$

where  $\mathbb{S}_{T,\ell}^{CSST}$  is in bps/Hz.

## Chapter 6

### RESULTS AND DISCUSSIONS

#### 6.1 Numerical and Simulation Results

We verify our theoretical results and present the results of a numerical study of the discussed FD OCNOMA system in this chapter. The graphic representations in this chapter demonstrate a good justification between the numerical results and simulation results, proving the accuracy of our work from the previous chapter 5. In this chapter, we set up the entire OCNOMA system with value  $K = 2$  to consist of several NOMA users, with  $U_0$  acting to be the PU and for SUs  $U_k$ ,  $k = 1, 2$ . Unless otherwise noted, we adjusted the parameters used in the system as listed in Table 1.

Parameter	Value
Average fading powers ( $\Omega_{su_0}, \Omega_{sr}, \Omega_{ru_0}, \Omega_{ru_1}, \Omega_{ru_2}$ )	0.1, 1, 0.7, 1, 1.3
Fading severity parameters ( $m_{su_0}, m_{sr}, m_{ru_0}, m_{ru_k}, m_{u_k}$ )	1, 2, 2, 2, 2
Mean of LI and IS channel power gains ( $\Omega_{rr}, \Omega_{u_k}$ )	0.891, 0.1
Level of HIs ( $\theta_{su_0} = \theta_{sr} = \theta_{ru_0} = \theta_{ru_k} = \theta_{rr} = \sqrt{2}\theta_0$ )	$\theta_0 = 0, 0.1, 0.2, 0.3$
TS parameter ( $\beta$ )	0.2
PS parameter ( $\rho$ )	0.8
Energy conversion factor ( $\eta$ )	0.75
Block duration ( $T$ )	1 sec
Target rate ( $r_{th}^p = r_{th}^s$ )	0.5 bps/Hz
Noise variance ( $\sigma^2$ )	1
Level of stairways conjecture ( $H$ )	50

**Table 1: Simulation Parameters**

##### 6.1.1 Performance Analysis of Primary Network

The OP performance graphs for the primary network are plotted with the FD CSST scheme under the corresponding TS and PS protocols in Figures 11 and 12. The curves are created by

taking into account both the ideal (perfect) hardware, where  $\theta_0 = 0$ , and the imperfect hardware, where  $\theta_0 = 0.2$  represents the level of HIs. With the given values of  $r_{th}^p$  and  $\theta_0$ , we, from the figures can validate that curves are well aligned with the simulated curves

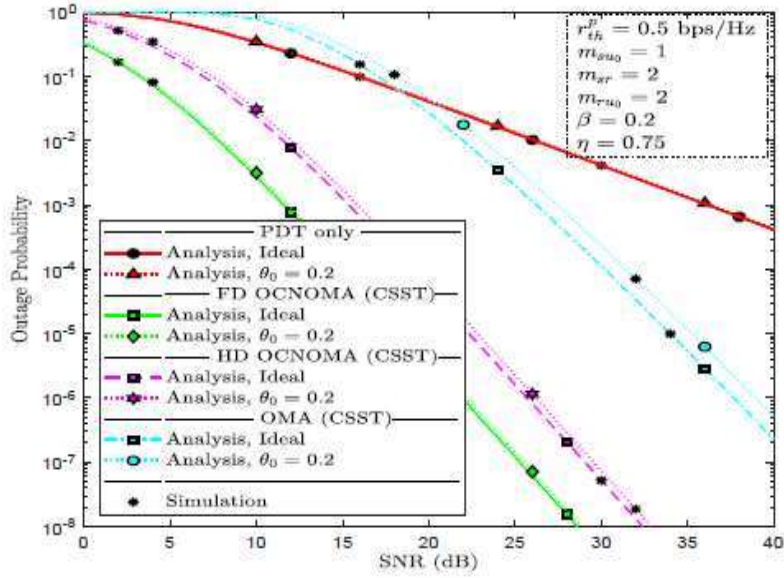


Figure 11: OP vs SNR for under TS protocol for primary network.

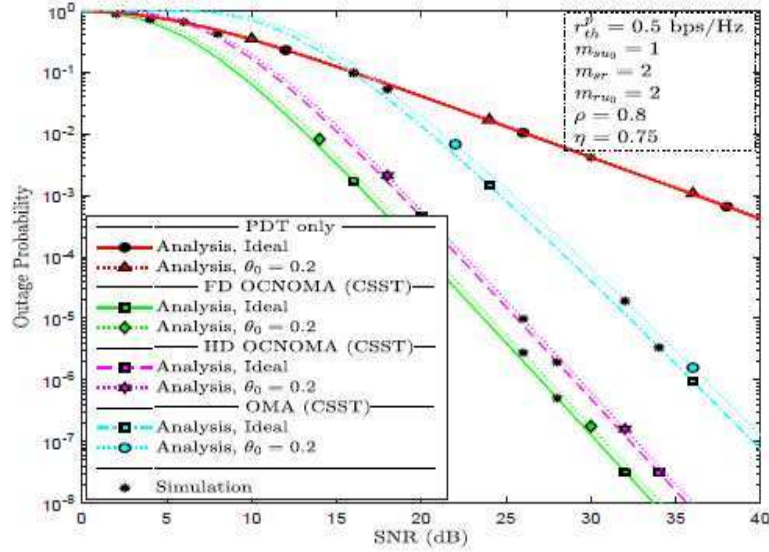


Figure 12: OP vs SNR for under PS protocol for primary network.

For the entire region of SNR. First, we observe that use of the CSST scheme for FD OCNOMA reveals a significantly lower OP in comparison of the DPT only scheme for the given target rate. Furthermore, the FD OCNOMA performs noticeably better than the OMA schemes and the competitive HD OCNOMA. Additionally, we observe that in the low SNR regime, the OMA-based CSST method performs the worst in terms of OP, while in the high the signal to noise ratio regime, it performs comparably better than the PDT scheme. As HIs ( $\theta_0 = 0.2$ ) are imposed, the OP outcomes of the CSST scheme deteriorates. Above all, comparing Figures 11 and 12 allows us to see that, under the specified set of conditions, the OP of the PS protocol deteriorates because of the lower received SINDR then the TS protocol.

### 6.1.2 Performance Analysis of Secondary Network

Using the derived mathematical equations from chapter 5, Fig. 13 shows the Outage Probability performance for a two-user secondary network using the TS based CSST scheme. To do this, we specifically plot the graphs for consumers  $U_1$  and  $U_2$  in the P-SIC and I-SIC scenarios, establishing the target rate values as  $r_{th}^p = r_{th}^s = 0.5$  bps /Hz In this instance, we take into account the amount of hardware impairments as  $\theta_0 = 0.3$ . Additionally, we visualize the graphs for the ideal scenario of flawless hardware ( $\theta_0 = 0$ ) for comparison's sake. Using the conditions covered in the previous section, we determined the corresponding values for  $\delta_0 = 0.6$ ,  $\delta_1 = 0.3$ , and  $\delta_2 = 0.1$  for FD OCNOMA power allocation, taking into account the highest priority of primary network user  $U_0$ . As anticipated, it is evident that the P-SIC has a significantly lower OP value in comparison to the I-SIC. It is evident that both users' OP performance declines as HIs increase, with the I-SIC case causing a more noticeable departure from ideal curve.

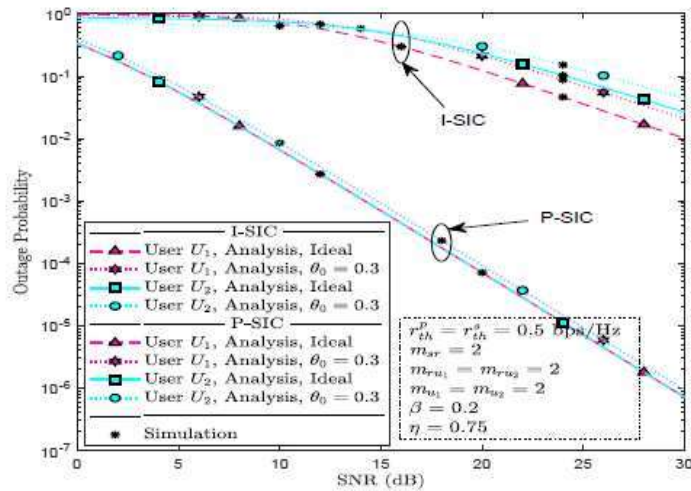


Figure 13: OP vs SNR of secondary network for the two-users.

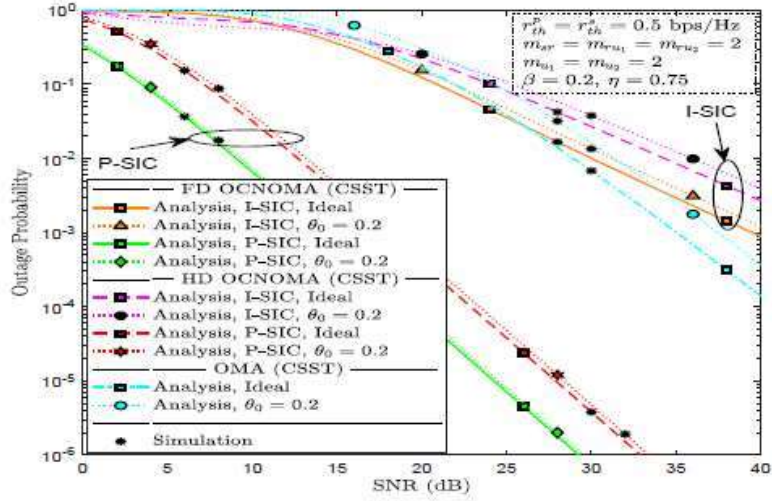


Figure 14: OP vs SNR under TS protocol secondary user ( $U_1$ ).

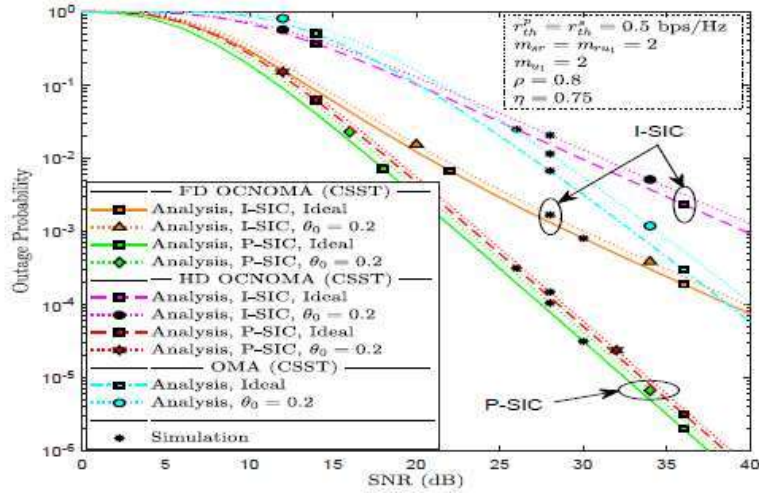


Figure 15: OP vs SNR under TS protocol secondary user ( $U_2$ ).

The Outage Probability performance of secondary network consumers  $U_1$  is being compared using the TS and PS protocols in Figures 14 and 15, respectively, under various relevant schemes. For this, we set the target rate as  $r_{th}^p = r_{th}^s = 0.5$  bps/Hz and HIs level as  $\theta_0 = 0, 0.2$ , and consider both P-SIC and I-SIC situations for CSST scheme. Thus, it is obvious that while the secondary network's Outage Probability performance deteriorates in I-SIC conditions for HD-based scheme, it intensifies under TS protocol. When compared to HD/FD-based CSST schemes, the performance degradation caused by HIs is more noticeable for OMA-based CSST schemes. Therefore, it can be argued that FD OCNOMA outperforms alternatives, even when considering the secondary network, and is more resistant to HIs.

### 6.1.3 Overall System Performance Analysis

Based on the analytical formula that was obtained in the preceding chapter 5, the system throughput graph in Fig. 16 finally provides an insight of the mean SE for the FD OCNOMA system. Here, we illustrate the TS and PS protocols' system throughput vs SNR curves for two distinct target rate values ( $r_{th}^p = r_{th}^s = 0.5$  bps/Hz and 0.8 bps/Hz). The relevant charts illustrate how the system throughput falls in the low SNR domain as the target rate rises. In contrast, the system throughput rises for the set goal rate up to a specific SNR value before becoming saturated. The maximum attainable throughput for the specified value of target is this saturated value. Throughput saturation for higher target rate values happens comparatively at high SNR. The reason for this is that the performance of the outage at a higher target rate is generally lower than the performance at a lower target rate. We can see from Fig. 16 that in the high SNR zone, the PS-based CSST scheme performs better in terms of throughput than the TS-based CSST method. This is to be expected, as PS provides a high SE while maintaining the effective IT time. For the PS protocol, this means that there is a trade-off between the increase in SE and the decrease in OP performance.

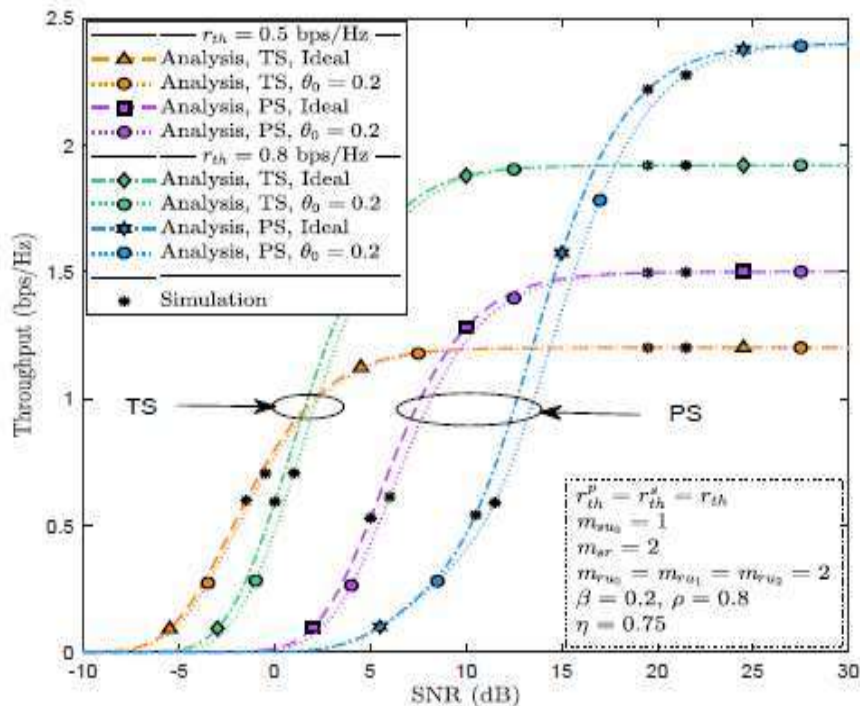
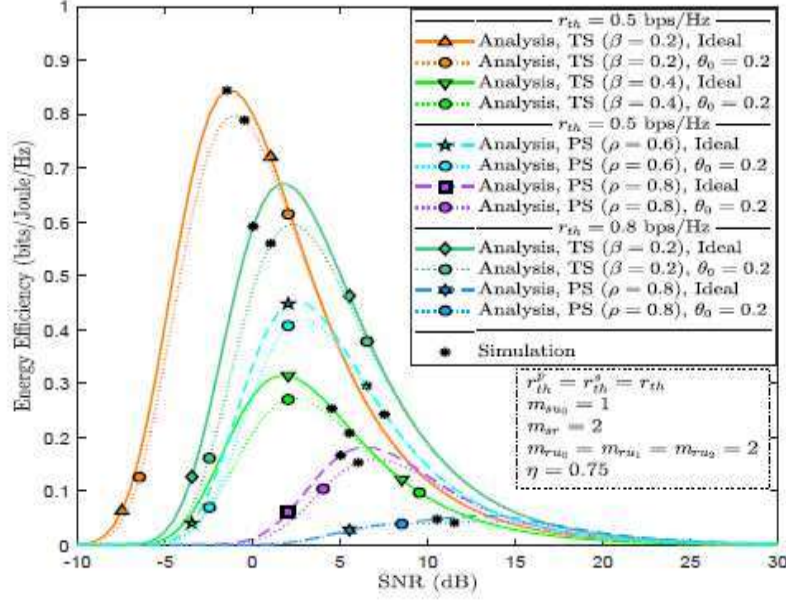


Figure 16: Plots of throughput vs SNR for the FD OCNOMA system.



**Figure 17: Plots of Energy efficiency vs SNR for FD OCNOMA system**

The energy efficiency for FD OCNOMA system under the TS and PS protocols is shown in Figure 17. For each of the two target rate values ( $r_{th}^p = r_{th}^s = 0.5$  bps/Hz and 0.8 bps/Hz), we plot the energy efficiency curves for our system with and without HIs against SNR. The relevant curves show that the system turns into less efficient in terms of energy at lower SNR values as we enhance the target rate. Examining two distinct HIs levels ( $\theta_0 = 0, 0.2$ ), it is evident that, in contrast to the optimal scenario, the energy efficiency of the system declines as HIs increases. This demonstrates how the imposition of HIs degrades energy efficiency performance. It is obvious from the persisted curves that the system attains the maximum energy efficiency during a given target rate and HI levels at a specific SNR value. The SNR value when the system reaches its greatest efficiency also varies if the target rate and HI levels change. As the SNR value rises, the considered system's energy efficiency falls. The obvious reason of this is higher power consumption than system throughput at higher SNR.

We also show, for specific target rate values and HIs levels, how the TS parameter and the PS parameter  $\beta$  and  $\rho$  respectively, affect the energy efficiency of system in Figure 17. It is obvious from the curves that system energy efficiency falls with increasing  $\beta$  or  $\rho$ . The reason being, as  $\beta$  value increases, the corresponding decrease in IT time causes a decrease in system throughput. Similarly, as  $\rho$  rises, the actual SINDR at the receiver decreases even though the IT time remains unchanged.

## **Chapter 7**

### **CONCLUSIONS AND FUTURE WORKS**

#### **7.1 Conclusions**

Using a PS/TS-based CSST technique in combination with PDT, we examined how the FD Multiuser OCNOMA system performed in relation to loop interference, I-SIC, and transceiver HIs. In particular, we used the FD-based CSST method to derive the mathematical equations of Outage probability for the primary and secondary networks under both the TS and PS protocols, and we evaluated the performance by adopting the Nakagami-m fading. The mathematical equations for system throughput and energy efficiency for the suggested FD OCNOMA system were given in order to provide additional understanding.

Most significantly, we proved that the suggested FD-based CSST method works noticeably better and is more resistant to HIs as compared to its HD counterparts. Our findings also showed that, although the TS-based CSST scheme would be more energy-efficient than the PS-based CSST scheme, the latter can achieve a greater throughput performance.

#### **7.2 Future Works**

There are a number of unresolved issues with growing 6G communication that are connected to the themes of this thesis and could be addressed in subsequent studies. The sequel provides a few potential directions for the research.

Spectral and high energy efficiency is a crucial goal for future networks. In this thesis by utilizing Multiple-input Multiple-output (MIMO) technology, the OCNOMA system's throughput and spectrum efficiency will be further increased. Multiple antennas are used at the transceiver nodes in MIMO systems to deliver a high data rate.

One of the biggest issues in building the 6G networks is dealing with security breaches, which are of utmost importance. Additionally, the OCNOMA system is vulnerable to security risks as a result of the coexistence of PUs and SUs. Therefore, it is crucial and intriguing to create the OCNOMA system's physical layer security strategies.

So, in this project we can incorporate various security methods as well as MIMO technology for future work.

## REFERENCES

- [1] S. Lee, R. Zhang, and K. Huang, "Opportunistic wireless energy harvesting in cognitive radio networks," *IEEE Trans. Wireless Commun.*, vol. 12, no. 9, pp. 4788–4799, Sep. 2013.
- [2] A. M. Akhtar, X. Wang, and L. Hanzo, "Synergistic spectrum sharing in 5G HetNets: A harmonized SDN-enabled approach," *IEEE Commun. Mag.*, vol. 54, no. 1, pp. 40–47, Jan. 2016.
- [3] X. Chen, W. Ni, X. Wang, and Y. Sun, "Optimal quality-of-service scheduling for energy-harvesting powered wireless communications," *IEEE Trans. Wireless Commun.*, vol. 15, no. 5, pp. 3269–3280, May 2016.
- [4] L. R. Varshney, "Transporting information and energy simultaneously," in *Proc. IEEE Int. Symp. Inf. Theory*, Toronto, ON, Canada, Jul. 2008, pp. 1612–1616.
- [5] X. Zhou, R. Zhang, and C. K. Ho, "Wireless information and power transfer: Architecture design and rate-energy tradeoff," *IEEE Trans. Commun.*, vol. 61, no. 11, pp. 4754–4767, Nov. 2013.
- [6] A. A. Nasir, X. Zhou, S. Durrani, and R. A. Kennedy, "Wireless-powered relays in cooperative communications: Time-switching relaying protocols and throughput analysis," *IEEE Trans. Commun.*, vol. 63, no. 5, pp. 1607–1622, May 2015.
- [7] S. Haykin, "Cognitive radio: Brain-empowered wireless communications," *IEEE J. Sel. Areas Commun.*, vol. 23, no. 2, pp. 201–220, Feb. 2005.
- [8] A. Goldsmith, S. A. Jafar, I. Maric, and S. Srinivasa, "Breaking spectrum gridlock with cognitive radios: An information theoretic perspective," *Proc. IEEE*, vol. 97, no. 5, pp. 894–914, May 2009.
- [9] D. T. Hoang, D. Niyato, P. Wang, and D. I. Kim, "Opportunistic channel access and RF energy harvesting in cognitive radio networks," *IEEE J. Sel. Areas Commun.*, vol. 32, no. 11, pp. 2039–2052, Nov. 2014.
- [10] Y. Liu, S. A. Mousavifar, Y. Deng, C. Leung, and M. ElKashlan, "Wireless energy harvesting in a cognitive relay network," *IEEE Trans. Wireless Commun.*, vol. 15, no. 4, pp. 2498–2508, Apr. 2016.
- [11] G. Zheng, Z. Ho, E. A. Jorswieck, and B. Ottersten, "Information and energy cooperation in cognitive radio networks," *IEEE Trans. Signal Process.*, vol. 62, no. 9, pp. 2290–2303, May 2014. [12] D. K. Verma, R. Y. Chang, and F.-T. Chien, "Energy-assisted decode-and-forward for energy harvesting cooperative cognitive networks," *IEEE Trans. Cogn. Commun. Netw.*,

vol. 3, no. 3, pp. 328–342, Sep. 2017.

[13] Z. Ding, X. Lei, G. K. Karagiannidis, R. Schober, J. Yuan, and V. K. Bhargava, “A survey on non-orthogonal multiple access for 5G networks: Research challenges and future trends,” *IEEE J. Sel. Areas Commun.*, vol. 35, no. 10, pp. 2181–2195, Oct. 2017.

[14] Z. Yang, Z. Ding, P. Fan, and N. Al-Dhahir, “A general power allocation scheme to guarantee quality of service in downlink and uplink NOMA systems,” *IEEE Trans. Wireless Commun.*, vol. 15, no. 11, pp. 7244–7257, Nov. 2016.

[15] L. Lv, J. Chen, Q. Ni, Z. Ding, and H. Jiang, “Cognitive non-orthogonal multiple access with cooperative relaying: A new wireless frontier for 5G spectrum sharing,” *IEEE Commun. Mag.*, vol. 56, no. 4, pp. 188–195, Apr. 2018.

[16] ZHONGXIANG WEI et al. Research Issues, Challenges, and Opportunities of Wireless Power Transfer-Aided Full-Duplex Relay Systems 2017

[17] XUN GUAN et al. Non orthogonal multiple access with phase predistortion in visible light communication 2016

[18] Full-Duplex Non-Orthogonal Multiple Access Cooperative Spectrum-Sharing Networks with Non-Linear Energy Harvesting by [Azar Hakimi et al. 2020](#)

[19] X. Liu and N. Ansari, “Green relay assisted D2D communications with dual batteries in heterogeneous cellular networks for IoT,” *IEEE Internet Things J.*, vol. 4, no. 5, pp. 1707-1715, Oct. 2017.

[20] H. Sun, Q. Wang, S. Ahmed, and R. Q. Hu, “Non-orthogonal multiple access in a mmWave based IoT wireless system with SWIPT,” in *Proc. Veh. Technol. Conf. (VTC Spring)*, Sydney, NSW, Australia, Jun. 2017, pp. 1-5.

[21] Z. Yang, W. Xu, Y. Pan, C. Pan, and M. Chen, “Energy efficient resource allocation in machine-to-machine communications with multiple access and energy harvesting for IoT,” *IEEE Internet Things J.*, vol. 5, no. 1, pp. 229- 245, Feb. 2018.

[22] D. S. Gurjar, H. H. Nguyen, and H. D. Tuan, “Wireless information and power transfer for IoT applications in overlay cognitive radio networks,” *IEEE Internet Things J.*, vol. 6, no. 2, pp. 3257-3270, Apr. 2019.

[23] Q. Li, X. Zhang, A. Pandharipande, X. Ge, and H. Gharavi, “An energy-aware retransmission approach in SWIPT-based cognitive relay systems,” *IEEE Trans. Cogn. Commun. Netw.*, vol. 5, no. 9, pp. 580-594, Sep. 2019.

[24] W. Lu et al., “SWIPT cooperative spectrum sharing for 6G-enabled cognitive IoT network,” *IEEE Internet Things J.*, Sep. 2020, doi: 10.1109/JIOT.2020.3026730

- [25] N. I. Miridakis, S. Arzykulov, T. A. Tsiftsis, G. Yang, and G. Nauryzbayev, "Green CR-NOMA: A new interweave energy harvesting transmission scheme for secondary access," in Proc. 16th Int. Symp. Wireless Commun. Systems (ISWCS), Aug. 2019, pp. 571-576.
- [26] D. Wang and S. Men, "Secure energy efficiency for NOMA based cognitive radio networks with nonlinear energy harvesting," IEEE Access, vol. 6, pp. 62707-62716, Oct. 2018.
- [27] F. Li, H. Jiang, R. Fan, and P. Tan, "Cognitive non-orthogonal multiple access with energy harvesting: An optimal resource allocation approach," IEEE Trans. Veh. Technol., vol. 68, no. 7, pp. 7080-7095, Jul. 2019.
- [28] Y. Yu, Z. Yang, Y. Wu, J. A. Hussein, W. -K. Jia, and Z. Dong, "Outage performance of NOMA in cooperative cognitive radio networks with SWIPT," IEEE Access, vol. 7, pp. 117308-117317, Sep. 2019.
- [29] T. -H. Vu and S. Kim, "Performance evaluation of power beacon-assisted wireless powered NOMA IoT-based systems," IEEE Internet Things J., vol. 8, no. 14, pp. 11655-11665, Jul. 2021.
- [30] D. K. P. Asiedu, S. Mahama, C. Song, D. Kim, and K.-J. Lee, "Beamforming and resource allocation for multi-user full-duplex wireless powered communications in IoT networks," IEEE Internet Things J., vol. 7, no. 12, pp. 11355-11370, Dec. 2020
- [31] X. Wang, M. Jia, Q. Guo, I. W.-H. Ho, and F. C.-M. Lau, "Full-duplex relaying cognitive radio network with cooperative nonorthogonal multiple access," IEEE Syst. J., vol. 13, no. 4, pp. 3897-3908, Dec. 2019.
- [32] I. S. Gradshteyn and I. M. Ryzhik, Tables of Integrals, Series and Products, 6th ed. New York: Academic Press, 2000